The Arabidopsis Endosomal Sorting Complex Required for Transport III Regulates Internal Vesicle Formation of the Prevacuolar Compartment and Is Required for Plant Development[1][C][W][OPEN]

Yi Cai[2,3], Xiaohong Zhuang[2], Caiji Gao[2], Xiangfeng Wang[2], and Liwen Jiang*

School of Life Sciences, Centre for Cell and Developmental Biology and State Key Laboratory of Agrobiotechnology, The Chinese University of Hong Kong, Shatin, New Territories, Hong Kong, China (Y.C., X.Z., C.G., X.W., L.J.); and Chinese University of Hong Kong Shenzhen Research Institute, The Chinese University of Hong Kong, Shenzhen 518057, China (L.J.)

ORCID ID: 0000-0002-2480-8210 (L.J.).

We have established an efficient transient expression system with several vacuolar reporters to study the roles of endosomal sorting complex required for transport (ESCRT)-III subunits in regulating the formation of intraluminal vesicles of prevacuolar compartments (PVCs)/multivesicular bodies (MVBs) in plant cells. By measuring the distributions of reporters on/within the membrane of PVC/MVB or tonoplast, we have identified dominant negative mutants of ESCRT-III subunits that affect membrane protein degradation from both secretory and endocytic pathways. In addition, induced expression of these mutants resulted in reduction in luminal vesicles of PVC/MVB, along with increased detection of membrane-attaching vesicles inside the PVC/MVB. Transgenic Arabidopsis (*Arabidopsis thaliana*) plants with induced expression of ESCRT-III dominant negative mutants also displayed severe cotyledon developmental defects with reduced cell size, loss of the central vacuole, and abnormal chloroplast development in mesophyll cells, pointing out an essential role of the ESCRT-III complex in postembryonic development in plants. Finally, membrane dissociation of ESCRT-III components is important for their biological functions and is regulated by direct interaction among Vacuolar Protein Sorting-Associated Protein20-1 (VPS20.1), Sucrose Nonfermenting7-1, VPS2.1, and the adenosine triphosphatase VPS4/SUPPRESSOR OF K^+ TRANSPORT GROWTH DEFECT1.

Endomembrane trafficking in plant cells is complicated such that secretory, endocytic, and recycling pathways are usually integrated with each other at the post-Golgi compartments, among which, the trans-Golgi network (TGN) and prevacuolar compartment (PVC)/multivesicular body (MVB) are best studied (Tse et al., 2004; Lam et al., 2007a, 2007b; Müller et al., 2007; Foresti and Denecke, 2008; Hwang, 2008; Otegui and Spitzer, 2008; Robinson et al., 2008; Richter et al., 2009; Ding et al., 2012; Gao et al., 2014). Following the endocytic trafficking of a lipophilic dye, FM4-64, the TGN and PVC/MVB are sequentially labeled and thus are defined as the early and late endosome, respectively, in plant cells (Lam et al., 2007a; Chow et al., 2008). While the TGN is a tubular vesicular-like structure that may include several different microdomains and fit its biological function as a sorting station (Chow et al., 2008; Kang et al., 2011), the PVC/MVB is 200 to 500 nm in size with multiple luminal vesicles of approximately 40 nm (Tse et al., 2004). Membrane cargoes destined for degradation are sequestered into these tiny luminal vesicles and delivered to the lumen of the lytic vacuole (LV) via direct fusion between the PVC/MVB and the LV (Spitzer et al., 2009; Viotti et al., 2010; Cai et al., 2012). Therefore, the PVC/MVB functions between the TGN and LV as an intermediate organelle and decides the fate of membrane cargoes in the LV.

In yeast (*Saccharomyces cerevisiae*), carboxypeptidase S (CPS) is synthesized as a type II integral membrane protein and sorted from the Golgi to the lumen of the vacuole (Spormann et al., 1992). Genetic analyses on the trafficking of CPS have led to the identification of approximately 17 class E genes (Piper et al., 1995; Babst et al., 1997, 2002a, 2002b; Odorizzi et al., 1998; Katzmann et al., 2001)

[1] This work was supported by the Research Grants Council of Hong Kong (grant nos. CUHK466610, 466011, 46112, 466613, CUHK2/CRF/11G, HKUST10/CRF/12R, HKBU1/CRF/10, and AoE/M-05/12), National Natural Science Foundation of China/Research Grants Council (grant no. N_CUHK406/12), National Natural Science Foundation of China (grant no. 31270226), and the Shenzhen Peacock Project (grant no. KQTD201101 to L.J.).

[2] These authors contributed equally to the article.

[3] Present address: Department of Molecular Biology and Centre for Computational and Integrative Biology, Massachusetts General Hospital, and Department of Genetics, Harvard Medical School, Boston, MA 02114.

* Address correspondence to ljiang@cuhk.edu.hk.

The author responsible for distribution of materials integral to the findings presented in this article in accordance with the policy described in the Instructions for Authors (www.plantphysiol.org) is: Liwen Jiang (ljiang@cuhk.edu.hk).

[C] Some figures in this article are displayed in color online but in black and white in the print edition.

[W] The online version of this article contains Web-only data.

[OPEN] Articles can be viewed online without a subscription.

www.plantphysiol.org/cgi/doi/10.1104/pp.114.238378

that constitute the core endosomal sorting complex required for transport (ESCRT) machinery. The evolutionarily conserved ESCRT complex consists of several functionally different subcomplexes, ESCRT-0, ESCRT-I, ESCRT-II, and ESCRT-III and the ESCRT-III-associated/Vacuolar Protein Sorting4 (VPS4) complex. Together, they form a complex protein-protein interaction network that coordinates sorting of cargoes and inward budding of the membrane on the MVB (Hurley and Hanson, 2010; Henne et al., 2011). Cargo proteins carrying ubiquitin signals are thought to be passed from one ESCRT subcomplex to the next, starting with their recognition by ESCRT-0 (Bilodeau et al., 2002, 2003; Hislop and von Zastrow, 2011; Le Bras et al., 2011; Shields and Piper, 2011; Urbé, 2011). ESCRT-0 recruits the ESCRT-I complex, a heterotetramer of VPS23, VPS28, VPS37, and MVB12, from the cytosol to the endosomal membrane (Katzmann et al., 2001, 2003). The C terminus of VPS28 interacts with the N terminus of VPS36, a member of the ESCRT-II complex (Kostelansky et al., 2006; Teo et al., 2006). Then, cargoes passed from ESCRT-I and ESCRT-II are concentrated in certain membrane domains of the endosome by ESCRT-III, which includes four coiled-coil proteins and is sufficient to induce the membrane invagination (Babst et al., 2002b; Saksena et al., 2009; Wollert et al., 2009). Finally, the ESCRT components are disassociated from the membrane by the adenosine triphosphatase (ATPase) associated with diverse cellular activities (AAA) VPS4/SUPPRESSOR OF K+ TRANSPORT GROWTH DEFECT1 (SKD1) before releasing the internal vesicles (Babst et al., 1997, 1998).

Putative homologs of ESCRT-I–ESCRT-III and ESCRT-III-associated components have been identified in plants, except for ESCRT-0, which is only present in Opisthokonta (Winter and Hauser, 2006; Leung et al., 2008; Schellmann and Pimpl, 2009). To date, only a few plant ESCRT components have been studied in detail. The Arabidopsis (*Arabidopsis thaliana*) AAA ATPase SKD1 localized to the PVC/MVB and showed ATPase activity that was regulated by Lysosomal Trafficking Regulator-Interacting Protein5, a plant homolog of Vps Twenty Associated1 Protein (Haas et al., 2007). Expression of the dominant negative form of SKD1 caused an increase in the size of the MVB and a reduction in the number of internal vesicles (Haas et al., 2007). This protein also contributes to the maintenance of the central vacuole and might be associated with cell cycle regulation, as leaf trichomes expressing its dominant negative mutant form lost the central vacuole and frequently contained multiple nuclei (Shahriari et al., 2010). Double null mutants of *CHARGED MULTIVESICULAR BODY PROTEIN*, *chmp1achmp1b*, displayed severe growth defects and were seedling lethal. This may be due to the

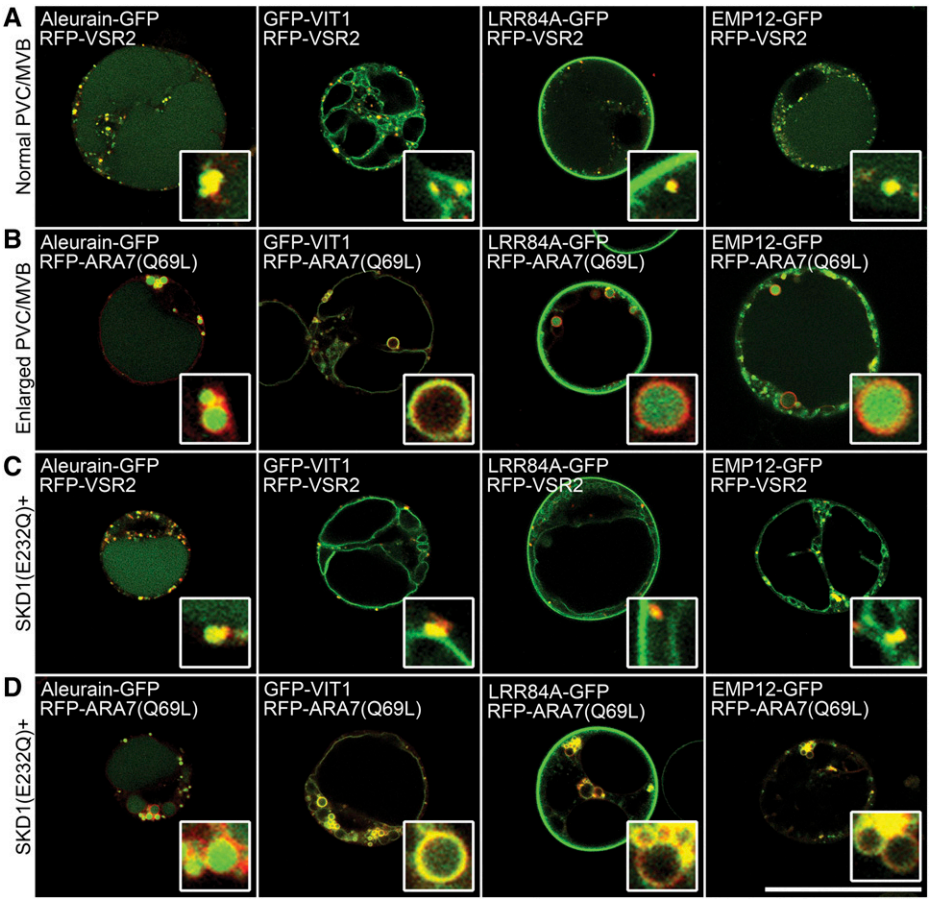

Figure 1. An efficient system with four vacuolar reporters to study the biogenesis of PVC/MVB's internal vesicles. Four reporters, a soluble vacuolar cargo aleurain-GFP, a tonoplast-localized iron transporter GFP-Vacuolar Iron Transporter1 (VIT1), and two degraded membrane proteins, Leucine-Rich-Repeat84A (LRR84A)-GFP and Endomembrane Protein12 (EMP12)-GFP, were used in this system. A and B, Coexpression of the four reporters with Red Fluorescent Protein (RFP)-Vacuolar Sorting Receptor2 (VSR2; A) or RFP-ARA7(Q69L; B) in Arabidopsis protoplasts. Note that the soluble vacuolar cargo aleurain-GFP as well as the degraded membrane proteins LRR84A-GFP and EMP12-GFP were trapped in the lumen of the enlarged PVC induced by RFP-ARA7(Q69L). C and D, Coexpression of the reporters with SKD1 (E232Q) and RFP-VSR2 (C) or RFP-ARA7(Q69L; D) in Arabidopsis protoplasts. Note that the soluble vacuolar cargo aleurain-GFP remained in the lumen of the enlarged PVC, whereas the degraded membrane proteins LRR84A-GFP and EMP12-GFP were colocalized with RFP-ARA7(Q69L) on the membrane of the enlarged PVC (D). Bar = 50 μm. [See online article for color version of this figure.]

mislocalization of plasma membrane (PM) proteins, including those involved in auxin transport such as PINFORMED1, PINFORMED2, and AUXIN-RESISTANT1, from the vacuolar degradation pathway to the tonoplast of the LV (Spitzer et al., 2009).

Plant ESCRT components usually contain several homologs, with the possibility of functional redundancy. Single mutants of individual ESCRT components may not result in an obvious phenotype, whereas knockout of all homologs of an ESCRT component by generating double or triple mutants may be lethal to the plant. As a first step to carry out systematic analysis on each ESCRT complex in plant cells, here, we established an efficient analysis system to monitor the localization changes of four vacuolar reporters that accumulate either in the lumen (LRR84A-GFP, EMP12-GFP, and aleurain-GFP) or on the tonoplast (GFP-VIT1) of the LV and identified several ESCRT-III dominant negative mutants. We reported that ESCRT-III subunits were involved in the release of PVC/MVB's internal vesicles from the limiting membrane and were required for membrane protein degradation from secretory and endocytic pathways. In addition, transgenic Arabidopsis plants with induced expression of ESCRT-III dominant negative mutants showed severe cotyledon developmental defects. We also showed that membrane dissociation of ESCRT-III subunits was regulated by direct interaction with SKD1.

RESULTS

An Efficient System to Study the Biogenesis of PVC/MVB's Internal Vesicles

A number of cargo proteins are processed for degradation by being engulfed into the luminal vesicles of the PVC/MVB before reaching the vacuole (Spitzer et al., 2009; Viotti et al., 2010; Cai et al., 2012; Gao et al., 2012). In this process, the evolutionarily conserved ESCRT machinery plays key roles in guiding the sorting of cargo proteins and inducing inward budding of the membrane (Hurley and Emr, 2006; Winter and Hauser, 2006). In plants, although several genetic and biochemical analyses have been carried out to fulfill the map of the ESCRT machinery (Spitzer et al., 2006, 2009; Haas et al., 2007; Shahriari et al., 2010, 2011; Richardson et al., 2011; Ibl et al., 2012), most of the plant ESCRT subunits remain functionally unknown, and systematic approach for understanding their functions in plant cells is still lacking. Thereby, we established an efficient transient expression system using Arabidopsis

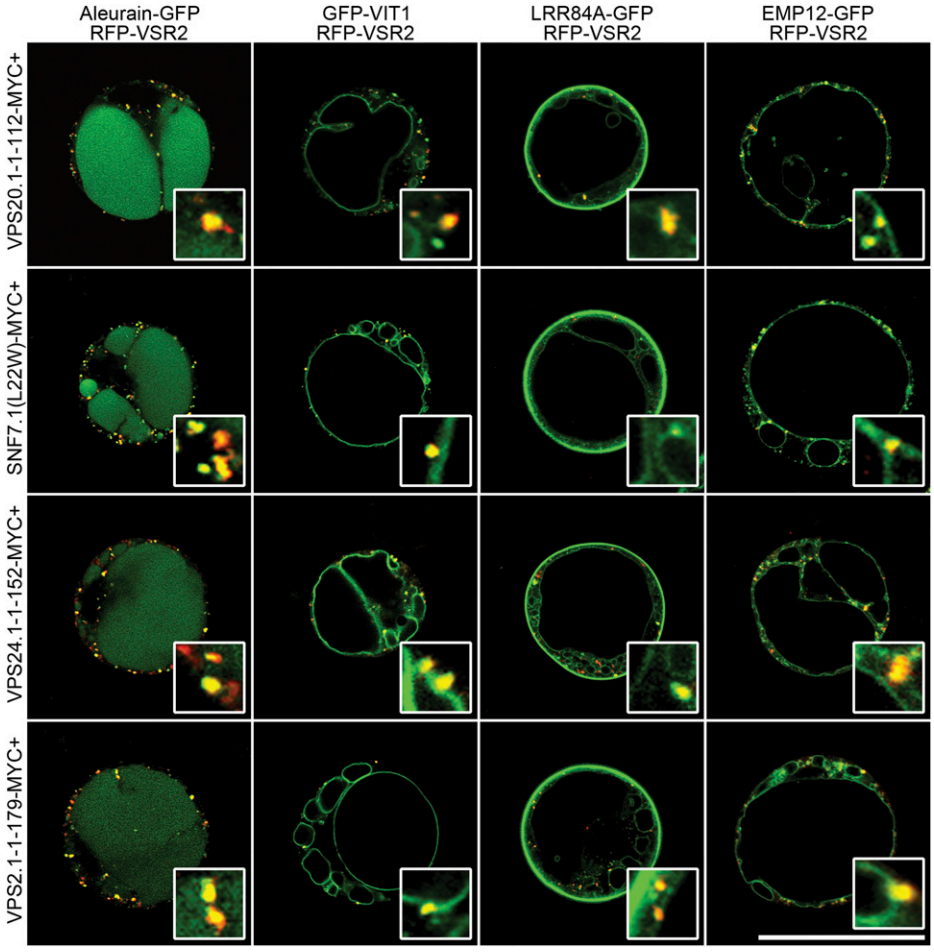

Figure 2. Overexpression of ESCRT-III dominant negative mutants altered the localizations of the reporters on the LV. A to D, Coexpression of the myc-tagged ESCRT-III dominant negative mutants with four reporters and RFP-VSR2 in Arabidopsis protoplasts. Bar = 50 μm. [See online article for color version of this figure.]

protoplasts to monitor the cellular functions of ESCRT machinery during the biogenesis of PVC/MVB's internal vesicles.

Four GFP fusions were selected and used as reporters for vacuolar targeting in this study (Fig. 1A): (1) LRR84A-GFP, a PM-localized LRR-Receptor-Like Kinase that undergoes internalization and proteolysis in the vacuole (Cai et al., 2012); (2) EMP12-GFP, an integral membrane protein that traffics through the Golgi apparatus prior to reaching the vacuole via TGN-PVC for degradation (Gao et al., 2012); (3) aleurain-GFP, a reporter for the lumen of the vacuole (Shen et al., 2013); and (4) GFP-VIT1, a membrane marker for the tonoplast (Kim et al., 2006). As shown in Figure 1A, all four fusions reached the vacuole via the RFP-VSR2-positive PVCs/MVBs, even though they accumulated in the lumen or tonoplast of the vacuole, respectively. To determine the site where the four reporters are separated from each other, RFP-ARA7(Q69L), a GTP-binding form of ARA7 that can enlarge the plant PVC/MVB (Kotzer et al., 2004; Jia et al., 2013; Cui et al., 2014), was coexpressed with the reporters. As expected, the GFP fusions showed distinct localizations on the enlarged PVC/MVB, with LRR84A-GFP, EMP12-GFP, and aleurain-GFP in the lumen and GFP-VIT1 on the outer membrane, indicating that LRR84A-GFP and EMP12-GFP were already relocated into the internal vesicles of the PVC/MVB before reaching the LV (Fig. 1B).

SKD1, an Arabidopsis homolog of the yeast and mammalian AAA ATPase VPS4/SKD1, is an ESCRT-III-associated protein that localizes to the cytoplasm and PVC/MVB. Overexpression of SKD1(E232Q), an ATPase-deficient form of SKD1, caused the enlargement of the PVC/MVB with a reduced number of luminal vesicles (Haas et al., 2007). This dominant negative mutant SKD1 (E232Q) was coexpressed with the four reporters to evaluate the transient expression system used in this study. As shown in Figure 1C, in protoplasts expressing SKD1(E232Q), LRR84A-GFP and EMP12-GFP changed their location from the lumen of the vacuole to the tonoplast, whereas the expression patterns of aleurain-GFP and GFP-VIT1 remained unchanged. To examine if the sorting event occurs on the PVC/MVB before these cargoes reach the vacuole, we coexpressed these reporters together with SKD1(E232Q) and RFP-ARA7(Q69L). As shown in Figure 1D, redistribution of LRR84A-GFP and EMP12-GFP took place at the PVC/MVB owing to the ability of SKD1(E232Q) to reduce the formation of PVC/MVB's internal vesicles (Haas et al., 2007). These results indicate that our transient expression system is

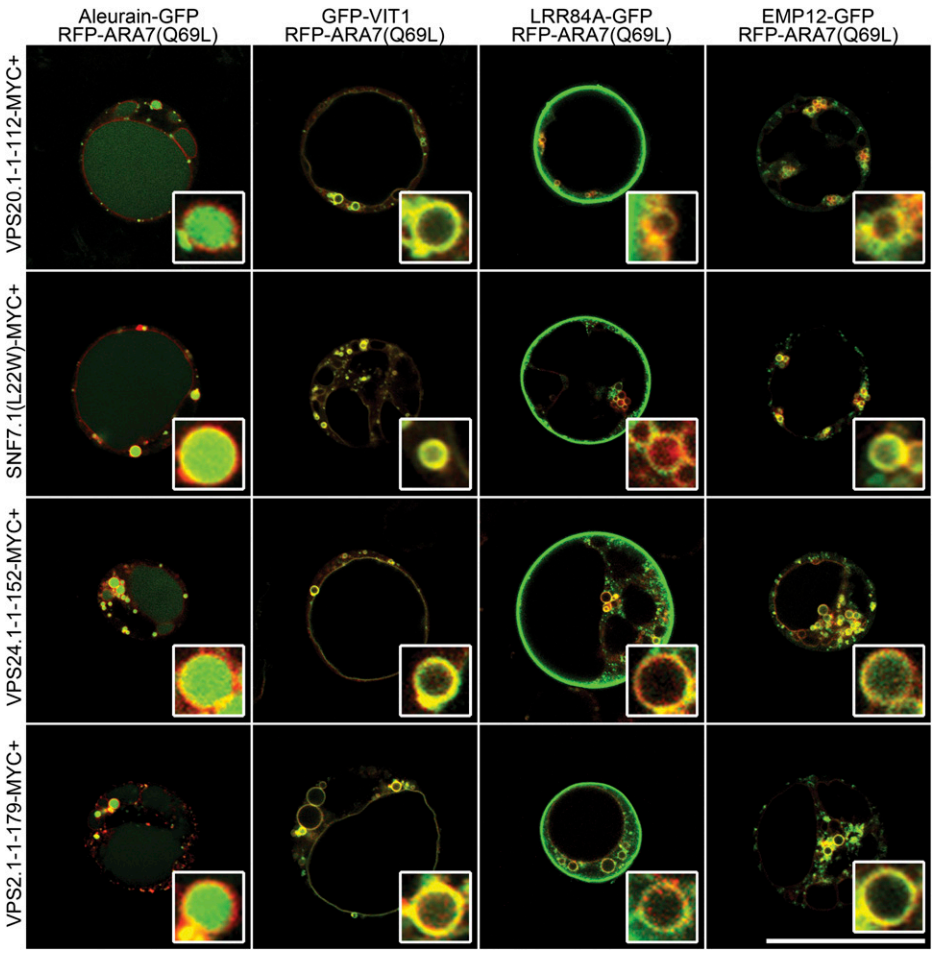

Figure 3. Overexpression of ESCRT-III dominant negative mutants altered the localizations of the reporters on the enlarged PVC/MVB. A to D, Coexpression of the myc-tagged ESCRT-III dominant negative mutants with four reporters and RFP-ARA7(Q69L) in Arabidopsis protoplasts. Bar = 50 μm. [See online article for color version of this figure.]

efficient for the systematic functional analysis of the ESCRT-III complex.

ESCRT-III Subunits Are Required for the Degradation of Membrane Proteins from Secretory and Endocytic Pathways

Numerous studies, including extensive genetic analyses and in vitro reconstitution of the ESCRT-III machinery in mammalian and yeast cells, have now highlighted the key roles of this subcomplex in PVC/MVB biogenesis (Babst et al., 2002a; Saksena et al., 2009; Wollert et al., 2009; Wollert and Hurley, 2010). Although all of the ESCRT-III subunits have been identified in Arabidopsis based on genome comparison and homology analysis (Winter and Hauser, 2006), with some data on their subcellular localizations and interactome (Richardson et al., 2011; Scheuring et al., 2011; Shahriari et al., 2011), their cellular functions remain unclear and the working model is still obscure.

XFP (for any kind of fluorescent protein) fusion approach has been widely used for detecting the subcellular localizations of ESCRT-III components in mammalian cells (Tsang et al., 2006; Ariumi et al., 2011; Guizetti et al., 2011; Carlton et al., 2012; Fumoto et al., 2012; Schiel et al., 2012) and in yeast (Teis et al., 2008, 2010; Davies et al., 2010; McMurray et al., 2011; Henne et al., 2012). Recent studies in plants also used the transient system by expressing the XFP fusions of ESCRT components to analyze their subcellular distributions (Katsiarimpa et al., 2011; Scheuring et al., 2011; Shahriari et al., 2011; Ibl et al., 2012). However, caution should be considered in using XFP fusions, and multiple approaches are needed to confirm the results (Denecke et al., 2012). For example, VPS2.2-GFP was shown to be a functional fusion that coimmunoprecipitated with other ESCRT proteins and complemented the *vps2.2* mutant (Ibl et al., 2012), whereby the *VPS2.1pro*:*Yellow Fluorescent Protein* (*YFP*)-*VPS2.1* construct only partially rescued the developmental arrest of *vps2.1* mutant embryos (Katsiarimpa et al., 2011). Moreover, while YFP-VPS2.1 diffused in the cytosol (Katsiarimpa et al., 2011), VPS2.1-YFP displayed a punctate distribution that partially colocalized with the PVC/MVB marker mRFP-VSR2 (Scheuring et al., 2011). Therefore, YFP tag was fused to the C terminus of ESCRT-III components and used in this study. Similar to previous reports (Katsiarimpa et al., 2011; Scheuring et al., 2011; Shahriari et al., 2011; Ibl et al., 2012), we first used a transient expression system to study the subcellular localizations of four putative Arabidopsis ESCRT-III subunits (VPS20.1, Sucrose Nonfermenting7-1 (SNF7.1), VPS24.1, and VPS2.1) using their YFP fusions. ESCRT-III YFP fusions were coexpressed with different organelle markers (Mannosidase1 (Man1)-RFP for the Golgi, RFP-Syntaxin of Plants61 (SYP61) for the TGN, RFP-VSR2 for the PVC/MVB, and RFP-ARA7(Q69L) for the enlarged PVC/MVB) in Arabidopsis protoplasts to observe their subcellular localizations. As shown in Supplemental Figures S1 to S4, while VPS24.1-YFP and VPS2.1-YFP showed high cytoplasmic expression pattern and an obscure colocalization with the PVC/MVB marker RFP-VSR2, SNF7.1-YFP did not show a clear colocalization and VPS20.1-YFP was mostly cytosolic. However, because the functionality of these fusion proteins was not tested in this study, it remains to be determined whether this C-terminal tagging approach might cause partial mislocalizations of these ESCRT-III proteins (Teis et al., 2008). In a recent study of ESCRT-III in Arabidopsis, VPS2.1-GFP fusion was shown to have a dominant negative effect, indicating that the partially functional impairment of this protein was likely caused by GFP tagging (Katsiarimpa et al., 2013). We also noted that SNF7.1-YFP and VPS2.1-YFP tended to form aggregates when excess plasmid DNA was added, and therefore, we applied a moderate amount of DNA (10 μg) in our studies (Supplemental Fig. S5).

Previous structural studies and in vivo functional analysis of mammalian and yeast ESCRT-III subunits have identified a set of dominant negative mutants

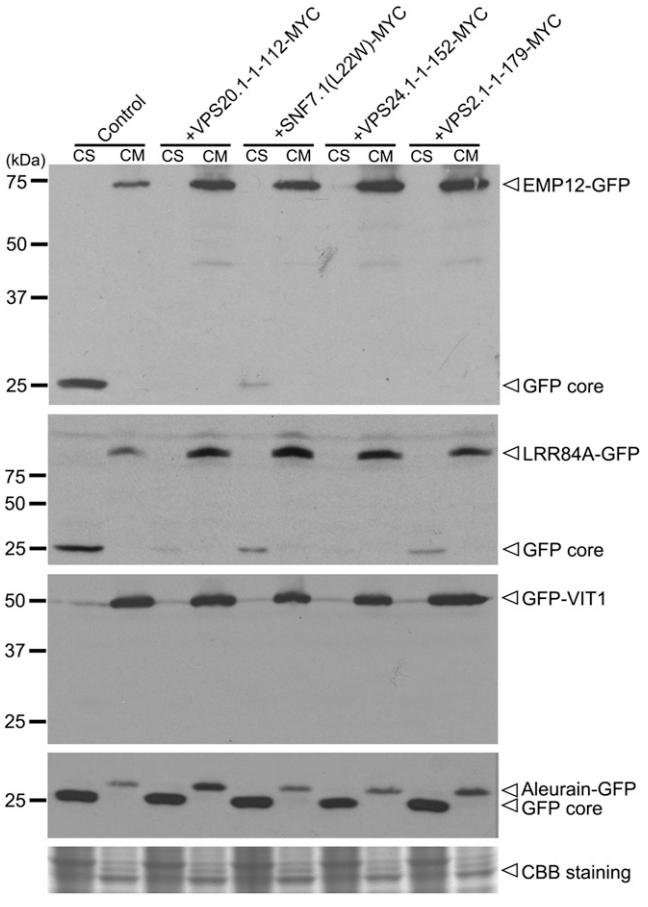

Figure 4. Western-blot analysis on the degradation of reporters in the presence of ESCRT-III dominant negative mutants. CS and CM fractions were isolated from transiently expressed Arabidopsis protoplasts and subjected to western-blot analysis to detect the effect of ESCRT-III dominant negative mutants on the degradation of EMP12-GFP, LRR84A-GFP, GFP-VIT1, and aleurain-GFP using GFP antibody. Coomassie Blue (CBB) staining was used as the loading control.

that affect the transport of PVC/MVB's luminal cargoes such as CPS (Dukes et al., 2008; Bajorek et al., 2009; Saksena et al., 2009). Based on this information and homology analysis, we generated dominant negative mutants of Arabidopsis ESCRT-III subunits and fused them with the MYC tag, a polypeptide tag derived from the c-myc oncogene. To test their functions, ESCRT-III mutants were next coexpressed with the four reporters in our transient expression system. As shown in Figures 2 and 3, similar to the effect of SKD1(E232Q), these mutants caused redistribution of the two PVC/MVB luminal cargoes LRR84A-GFP and EMP12-GFP to the tonoplast and outer membrane of the enlarged PVC/MVB, whereas coexpression of wild-type ESCRT-III

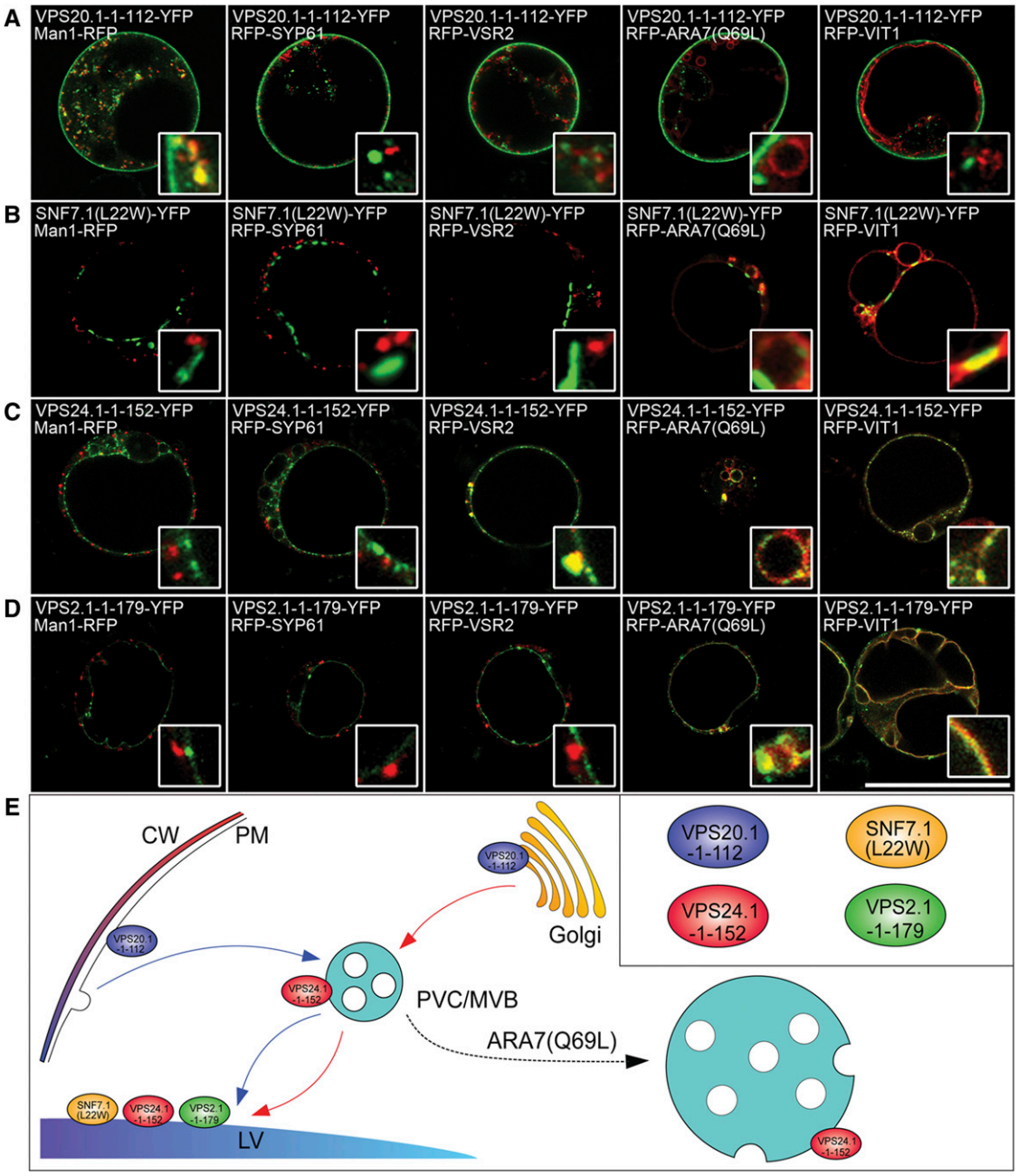

Figure 5. Subcellular localizations of ESCRT-III mutant YFP fusions. A to D, VPS20.1-1-112-YFP, SNF7.1(L22W)-YFP, VPS24.1-1-152-YFP, or VPS2.1-1-179-YFP was coexpressed with different organelle markers including the Golgi marker Man1-RFP, the TGN marker RFP-SYP61, the PVC marker RFP-VSR2, the enlarged PVC marker RFP-ARA7(Q69L), and the tonoplast marker RFP-VIT1 in Arabidopsis protoplasts. Bar = 50 μm. E, Schematic model showing the subcellular localizations of ESCRT-III mutants. [See online article for color version of this figure.]

subunits did not alter the expression patterns of these reporters (Supplemental Figs. S6 and S7). When statistical analysis was performed, a majority of the protoplasts expressing ESCRT-III mutants displayed altered expression patterns of LRR84A-GFP and EMP12-GFP from the lumen of the LV to the tonoplast (Supplemental Fig. S8). Notably, none of the protoplasts showed tonoplast patterns in the control experiments (Supplemental Fig. S8). Interestingly, combinational expression of aleurain-GFP and RFP-VSR2 showed many green-only and red-only dots in addition to the yellow puncta (Figs. 1 and 2), supporting the notion that the PVCs fall into two or perhaps more classes (Foresti et al., 2010). When similar experiments were conducted in tobacco (*Nicotiana tabacum*) BY-2 (Bright Yellow2) cells, all ESCRT-III dominant negative mutants caused redistribution of EMP12-GFP from the lumen of the vacuole to the tonoplast (Supplemental Fig. S9). Therefore, conserved ESCRT-III machinery may also functionally operate in tobacco BY-2 cells.

To further verify the above confocal data, cell-soluble (CS) or cell membrane (CM) fractions isolated from transiently expressed protoplasts were examined by western blot to follow the fate of the reporters. As shown in Figure 4, a 25-kD band accumulated in the control CS fraction that represented the classical vacuolar degraded products of the GFP fusions (Frigerio et al., 2001; Brandizzi et al., 2002; daSilva et al., 2005, 2006; Cai et al., 2012). In samples prepared from protoplasts overexpressing ESCRT-III dominant negative mutants, accumulation of the GFP core in the CS fraction was greatly reduced compared with the control lanes (Fig. 4). Taken together, these data suggested that functional ESCRT-III subunits were required for PVC/MVB internalization and LV degradation of cargo proteins from secretory and endocytic pathways (Figs. 2–4). We also noticed that the full length of soluble marker aleurain-GFP substantially appeared in the membrane fraction. After overnight expression of aleurain-GFP, most of the GFP signals (likely the GFP core) were accumulated in the vacuole, while the full-length aleurain-GFP proteins remained intact in various compartments, such as the Golgi apparatus, TGN, and PVC/MVB, during their transport to the vacuole. In addition, during the simple fractionation procedure used in this study, most of these organelles might remain intact, and therefore, their luminal contents, such as aleurain-GFP proteins, were detected in the membrane fraction.

Mislocalization of Dominant Negative ESCRT-III Mutants

To further gain insight into how ESCRT-III dominant negative mutants interfere with the endogenous ESCRT-III machinery, we next carried out subcellular localization analysis on the ESCRT-III mutants. As shown in Figure 5C, terminus deletion caused redistribution of VPS2.1 from the PVC/MVB to the tonoplast, while SNF7.1 (L22W)-YFP and VPS24.1-1-152-YFP remained mostly punctate along the tonoplast, suggesting that the mutants were defective in membrane dissociation and thus

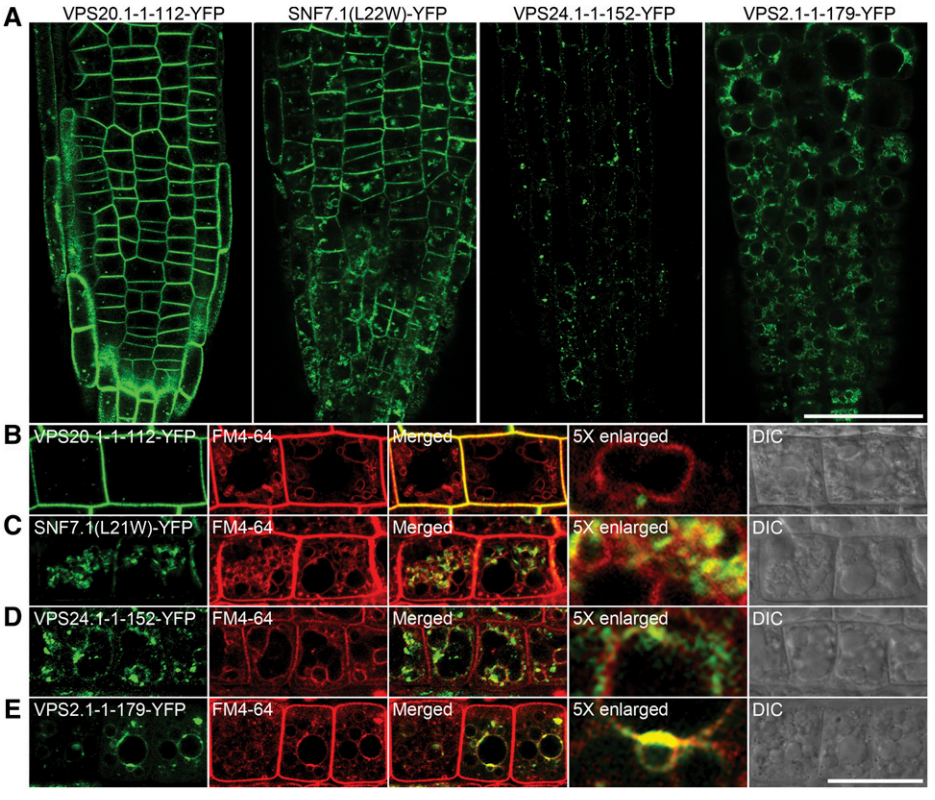

Figure 6. Induced expression patterns of ESCRT-III mutant YFP fusions in Arabidopsis root cells. A, Six-day-old transgenic Arabidopsis plants were transferred onto medium containing 10 μM β-estradiol for 24 h to induce the expression of ESCRT-III mutant YFP fusions. Bar = 50 μm. B to E, Transgenic Arabidopsis plants with induced expression of ESCRT-III mutant YFP fusions were labeled with FM4-64 for 4 h before confocal imaging to highlight the tonoplast staining. Bar = 25 μm. [See online article for color version of this figure.]

reached the LV when the PVC/MVB fused with the LV (Scheuring et al., 2011). This observation supported the notion that such mutations or deletions of ESCRT-III subunits enhanced their membrane association (Bajorek et al., 2009; Weiss et al., 2009). Particularly, truncation of VPS20.1 (VPS20.1-1-112) resulted in a different localization, with most of the YFP signals located on the PM (Fig. 5A). Because VPS20 initiates the recruitment of the ESCRT-III complex (Teis et al., 2008), we hypothesized that subsequent components of ESCRT-III may also be translocated to the PM together with the VPS20 mutant. When VPS20.1-1-112-MYC was coexpressed with ESCRT-III YFP fusions, VPS20.1-1-112-MYC caused redistribution of VPS20.1-YFP and SNF7.1-YFP to the PM (Supplemental Fig. S10A). When VPS20.1-1-112-RFP was coexpressed with VPS20.1-YFP or SNF7.1-YFP, these fusion proteins colocalized with each other on the PM and intracellular compartments (Supplemental Fig. S10, B and C). This observation was consistent with previous yeast two-hybrid analysis, which showed the self-interaction of VPS20.1 and the interaction between VPS20.1 and SNF7.1 (Richardson et al., 2011; Shahriari et al., 2011). Therefore, it was likely that VPS20.1-1-112 affected the locations and functions of endogenous VPS20.1 and SNF7.1, which, in turn, disrupted the proper translocation of other ESCRT-III subunits onto the PVC/MVB membrane for cargo sorting. The N-terminal a1/a2 hairpin of VPS20 has been proved to be sufficient to recruit SNF7-GFP to endosomes in yeast cells (Teis et al., 2008, 2010; Davies et al., 2010; McMurray et al., 2011; Henne et al., 2012).

Expression of Dominant Negative ESCRT-III Mutants Reduces the Number of Internal Vesicles within the PVCs/MVBs

To confirm our previous observations in transiently expressed Arabidopsis protoplasts, we have generated transgenic Arabidopsis plants by expressing ESCRT-III dominant negative mutants under the control of the β-estradiol-inducible system (Zuo et al., 2000; Liang et al., 2012). Six-day-old seedlings were transferred onto medium containing β-estradiol and incubated for 24 h to induce the expression of ESCRT-III mutants (Fig. 6A). Consistent with our previous observations, VPS2.1-1-179-YFP was found to colocalize with the endocytic tracker FM4-64 on the vacuolar membrane at 4 h after uptake in Arabidopsis root cells (Fig. 6E). We also noted that SNF7.1(L22W)-YFP showed additional signals on the PM in Arabidopsis root cells (Fig. 6, A and C).

Next, the role of ESCRT-III dominant negative mutants in the formation of PVC/MVB's internal vesicles was examined by analyzing the ultrastructure of the PVC/MVB. Vacuolar sorting receptors (VSRs) are type I integral transmembrane protein markers for the PVCs/MVBs (Tse et al., 2004). When coexpressed with the ESCRT-III mutants, VSR markers remained on the membrane of the

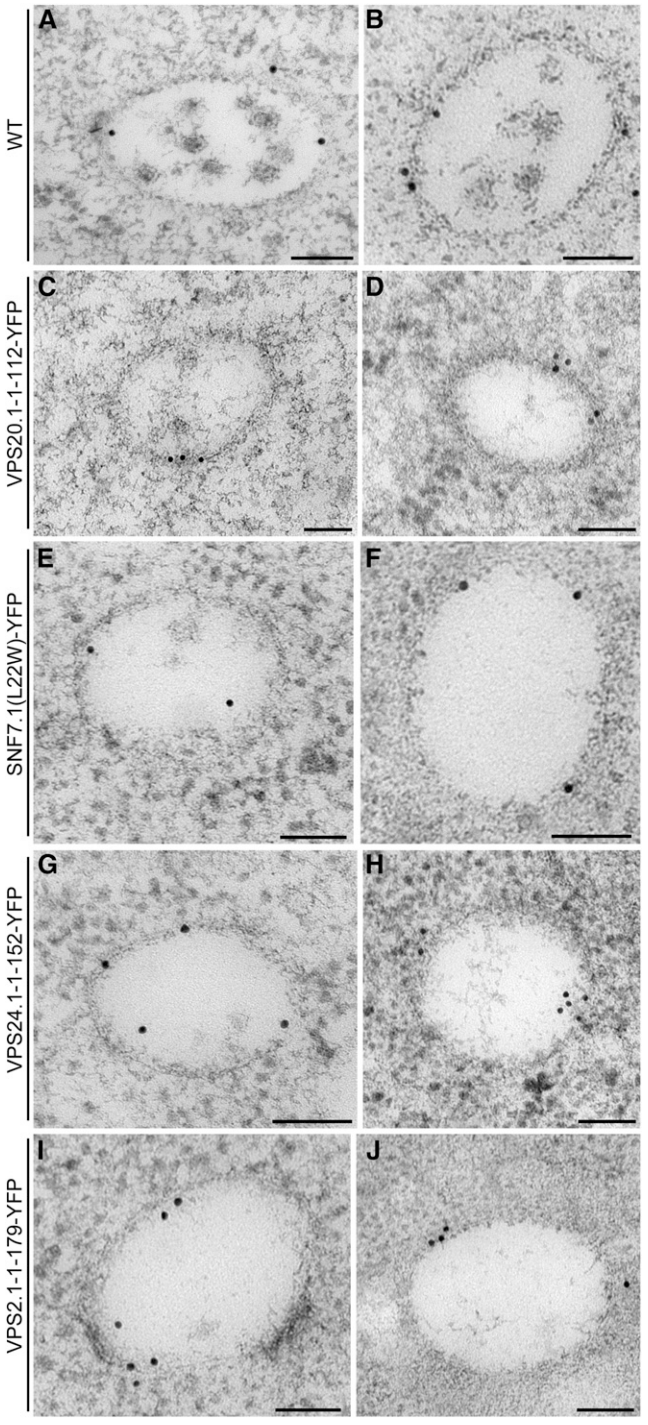

Figure 7. Immunogold detection of VSRs in wild-type and transgenic Arabidopsis plants with induced expression of ESCRT-III mutants. Six-day-old wild-type plants (A and B) and transgenic plants (C–J) germinated and cultured in the absence of inducers were transferred onto medium containing 10 μM β-estradiol for 24 h to induce the expression of VPS20.1-1-112-YFP (C and D), SNF7.1(L22W)-YFP (E and F), VPS24.1-1-152-YFP (G and H), or VPS2.1-1-179-YFP (I and J). Arabidopsis roots were subjected to high-pressure frozen/freeze substitution followed by ultrathin sectioning and immunogold labeling using VSR antibodies. Bar = 100 nm.

Table I. *Quantitative analysis of PVC/MVB structural characteristics in roots*

Only those endosomes labeled with the anti-VSR antibodies were used for this analysis.

Wild-type or Transgenic Plants Expressing ESCRT-III Mutants	PVC/MVB Diameter	No. of Luminal Vesicles per PVC/MVB	Percentage of Luminal Vesicles Attached to PVC/MVB Membrane	Diameter of Luminal Vesicles
	nm		%	*nm*
VPS20.1-1-112-YFP	310.6 ± 44.9 (n = 55)	0.2 ± 0.5	43.8	34.3 ± 3.4 (n = 14)
SNF7.1(L22W)-YFP	304.2 ± 42.8 (n = 46)	1.3 ± 1.7	38.7	39.6 ± 5.4 (n = 61)
VPS24.1-1-152-YFP	308.4 ± 47.4 (n = 44)	0.3 ± 0.8	35.7	37.1 ± 6.4 (n = 11)
VPS2.1-1-179-YFP	359.8 ± 68.7 (n = 89)	0.4 ± 1.1	66.2	46.5 ± 9.5 (n = 26)
Wild type	276.2 ± 15.2 (n = 32)	5.6 ± 1.2	9.9	36.0 ± 2.1 (n = 180)

ARA7(Q69L)-induced enlarged PVCs/MVBs (Supplemental Fig. S11). Because not all of the ESCRT-III dominant negative mutants localized to the PVCs/MVBs, we next used specific VSR antibodies for the identification of PVCs/MVBs in different mutant backgrounds (Fig. 7). Our results showed that in transgenic plants with induced expression of ESCRT-III dominant negative mutants, the number of PVC/MVB's internal vesicles was dramatically reduced and many PVCs/MVBs contained no internal vesicles (Fig. 7, D, F, H, and J). When a quantitative analysis on labeled PVCs/MVBs was performed, a higher proportion of vesicles was found to remain attached to the limiting membrane of the PVC/MVB, indicating that ESCRT-III dominant negative mutants delayed or inhibited the release of PVC/MVB's internal vesicles (Table I). Furthermore, we did not notice a prominent effect of dominant negative mutants on the size of the PVCs/MVBs and their luminal vesicles.

Expression of Dominant Negative ESCRT-III Mutants Causes Cotyledon Developmental Defects

To further understand the function of ESCRT-III components in plant development, wild-type or transgenic Arabidopsis plants were directly grown on the medium with or without inducer. Transgenic Arabidopsis plants showed normal growth phenotype in medium without inducer; however, upon the induced expression of ESCRT-III mutants, they displayed obvious cotyledon developmental defects when compared with the wild-type plants (Fig. 8A; Supplemental Fig. S12). To have a more detailed analysis, cotyledons from wild-type or transgenic Arabidopsis seedlings were glutaraldehyde/osmium tetroxide fixed and embedded in Spurr's resin for subsequent transmission electron microscopy analysis. As shown in Figure 8, in contrast to wild-type cells, most of the cotyledon mesophyll cells in transgenic Arabidopsis plants expressing ESCRT-III dominant negative mutants displayed a reduced cell size and lost the large central vacuole (Fig. 8, B and D). In addition, the plastids were unable to develop into normal chloroplasts with stacks of thylakoid for photosynthesis (Fig. 8C). The molecular mechanism of these ESCRT-III dominant negative mutants in inhibiting the formation of central vacuole and development of chloroplast in cotyledons remains unknown. One possibility is that postembryonic development of cotyledons in these mutants was disrupted at very early stage, pointing to an important role of ESCRT-III components in plant development.

SKD1 Directly Interacts with ESCRT-III Subunits and Regulates Their Membrane Dissociation

The AAA ATPase VPS4/SKD1 has long been viewed as a master regulator of membrane dissociation for the ESCRT-III subunits, and its ATP hydrolysis mutant induced the formation of class E compartments (Stuchell-Brereton et al., 2007; Azmi et al., 2008). In plants, previous studies also showed an interaction among VPS20.1, VPS2.1, and SKD1, suggesting a relationship between ESCRT-III components and SKD1 (Katsiarimpa et al., 2011; Richardson et al., 2011). Here, to further integrate this study with previous reports of plant ESCRT (Haas et al., 2007; Shahriari et al., 2010), we next studied the effects of SKD1(E232Q) mutant on the distribution of plant ESCRT-III subunits. As shown in Figure 9A, coexpression of SKD1(E232Q) caused the relocation of ESCRT-III subunits into aggregates, while no such effect was observed with the components of ESCRT-I (VPS28a-GFP) and ESCRT-II (VPS25-GFP). Moreover, the intracellular ESCRT-III YFP signals colocalized with RFP-SKD1(E232Q), suggesting that SKD1(E232Q) recruited ESCRT-III subunits to the class E compartments or enlarged PVCs/MVBs in plant cells (Haas et al., 2007; Katsiarimpa et al., 2011).

To further confirm the confocal observations, ESCRT-III YFP fusions or members of the ESCRT-I (VPS28a-GFP) and ESCRT-II (VPS25-GFP) complexes were coexpressed with SKD1(E232Q), followed by protein extraction and western-blot analysis using GFP antibodies to detect the fusion proteins. As shown in Figure 9B, SKD1(E232Q) specifically induced the redistribution of ESCRT-III components, especially VPS24.1 and VPS2.1, from the CS fraction to the CM fraction, suggesting an enhanced membrane association of ESCRT-III subunits upon SKD1(E232Q) coexpression.

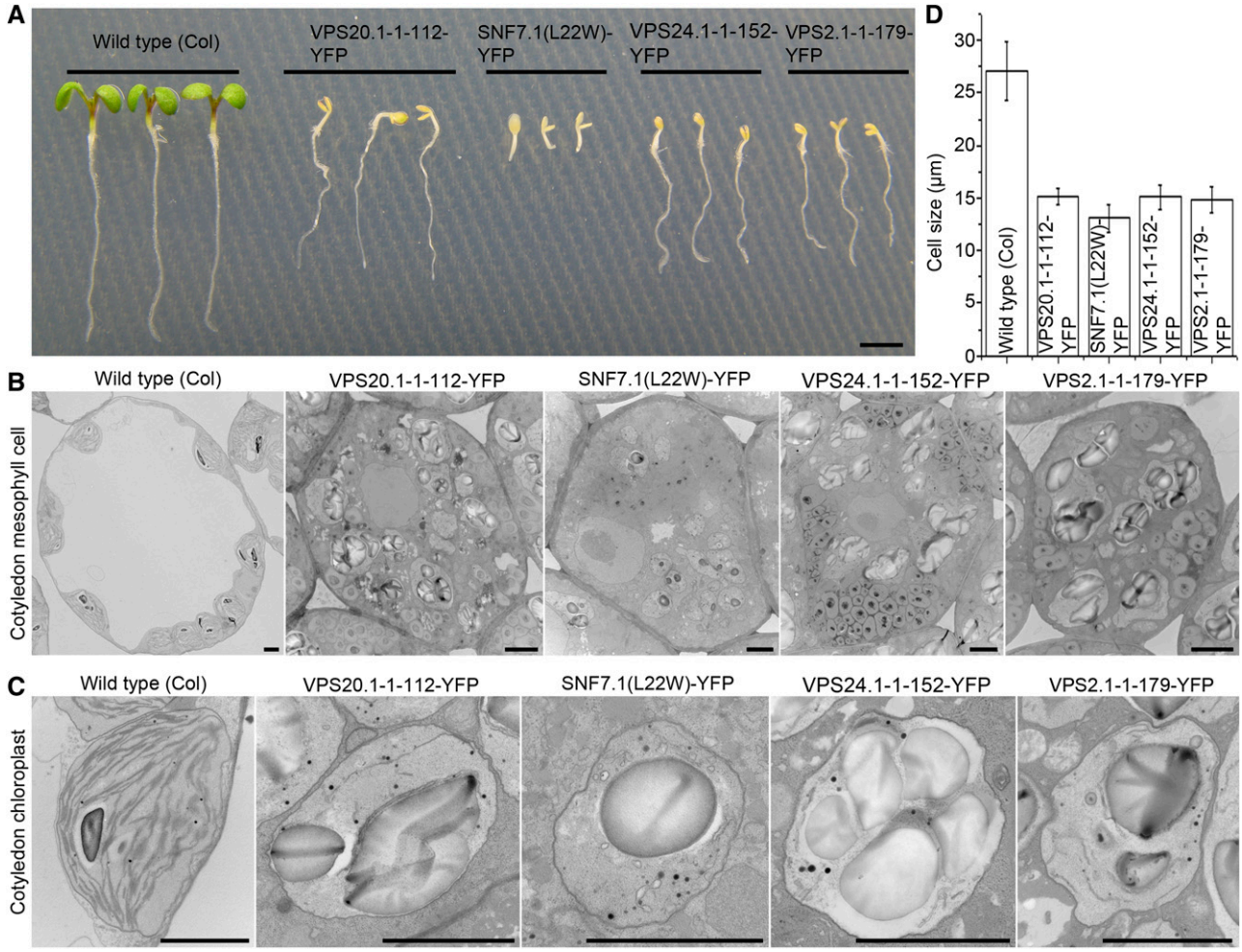

Figure 8. Induced expression of ESCRT-III mutant components caused developmental defects. A, Phenotypes of 6-d-old wild-type and transgenic Arabidopsis plants with induced expression of ESCRT-III dominant negative mutants grown in the presence of 1 μM β-estradiol. Bar = 2 mm. B and C, Morphological changes of mesophyll cells (B) and chloroplasts (C) in the cotyledons of 6-d-old wild-type or transgenic Arabidopsis plants with induced expression of ESCRT-III dominant negative mutants. Note the absence of the large central vacuoles and thylakoid membrane stacks in the transgenic plants expressing the ESCRT-III dominant negative mutants. Bar = 2 μm. D, Quantitative analysis of the cotyledon mesophyll cell size in wild-type or transgenic plants with induced expression of ESCRT-III dominant negative mutants. [See online article for color version of this figure.]

Because SKD1(E232Q) and ESCRT-III subunits localized to the same compartments when coexpressed, we therefore performed fluorescence resonance energy transfer (FRET) analysis to detect their physical interactions. In this study, free CFP and YFP proteins were expressed together as the negative control, while single expression of the CFP-YFP tandem fusion was used as the positive control (Supplemental Fig. S13; Shah et al., 2001, 2002). As shown in Supplemental Figure S13, our data clearly indicated that SKD1(E232Q) directly interacted with members of the ESCRT-III complex, VPS20.1, SNF7.1, and VPS2.1.

DISCUSSION

Conserved ESCRT-III Machinery in Plant Cells

The plant PVC/MVB, which is 200 to 500 nm in size, contains multiple luminal vesicles and functions as an intermediate station for cargoes on the way to the LV. These cargoes include transporters that function on the LV (e.g. Inositol Transporter1, VIT1, and Peptide Transporter2/Nitrate Transporter1) and transmembrane PM proteins (e.g. PINFORMED1, Brassinosteroid-Insensitive1, Boron Transporter1, OsSCAMP1 [for *Oryza sativa* secretory carrier membrane protein1], and LRR84A) destined for vacuolar degradation (Spitzer et al., 2009; Viotti et al., 2010; Cai et al., 2012; Komarova et al., 2012; Larisch et al., 2012; Wolfenstetter et al., 2012). Therefore, physical separation of these cargo proteins on the PVC/MVB is essential for their proper targeting to the LV. In mammalian and yeast cells, protein sorting and membrane isolation on the MVB are accomplished by the sequential actions of several protein complexes, ESCRT-0, ESCRT-I, ESCRT-II, and ESCRT-III plus the ESCRT-III-associated/VPS4 complex (Babst et al., 2002a, 2002b; Katzmann et al., 2003; Wollert and Hurley, 2010).

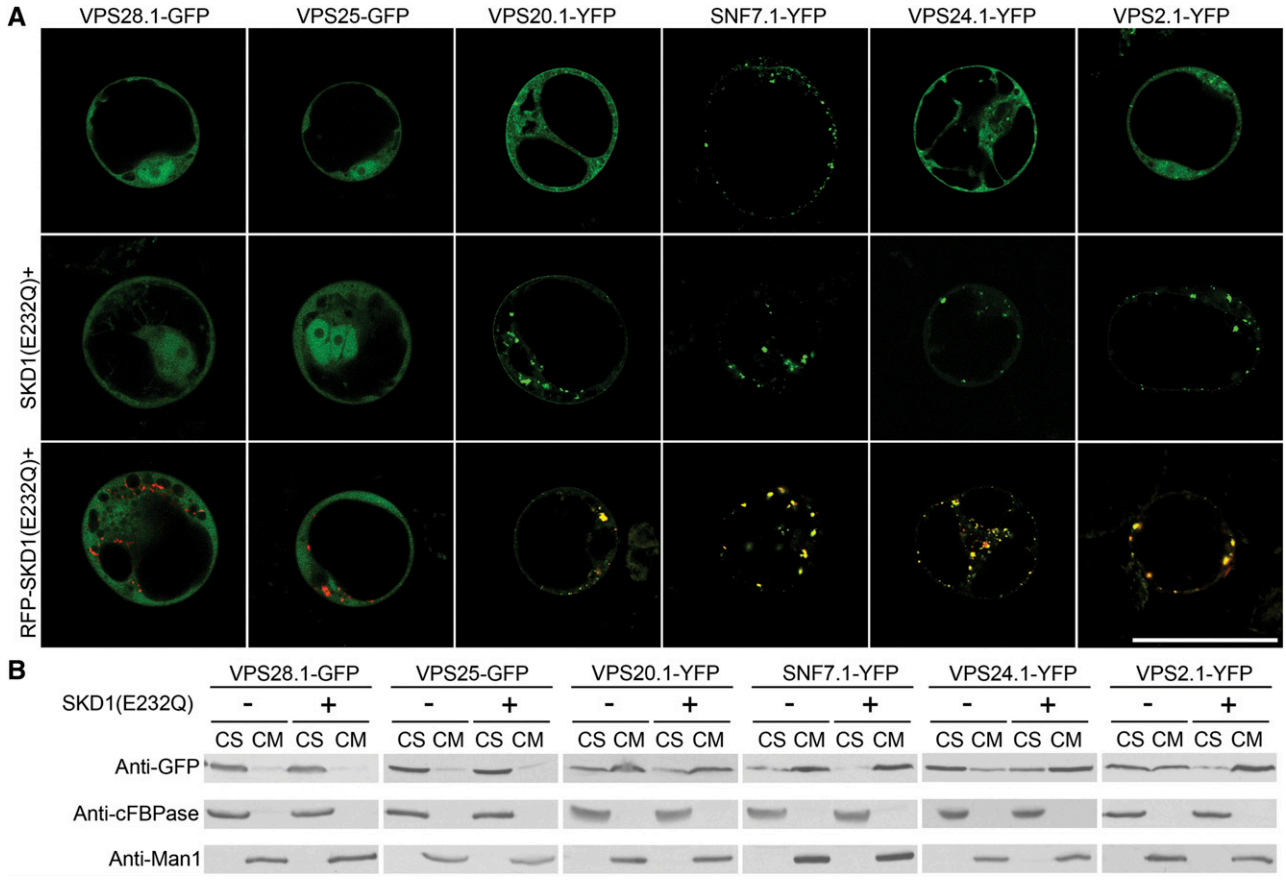

Figure 9. SKD1 regulated membrane disassociation of ESCRT-III but not ESCRT-I–ESCRT-II subunits. A, ESCRT-I–ESCRT-III subunits were coexpressed with SKD1(E232Q) or RFP-SKD1(E232Q) in Arabidopsis protoplasts. Bar = 50 μm. B, Western-blot analysis of the distribution of ESCRT-I–ESCRT-III subunits in the cytosol (CS) or on the membrane (CM) in the presence or absence of SKD1(E232Q). Arabidopsis protoplasts expressing the indicated constructs were subjected to protein isolation into CS and CM fractions, followed by protein immunoblot analysis using a GFP antibody, cytosolic fructose-1,6-bisphosphatase (cFBPase) antibody (CS fraction loading control), and Man1 antibody (CM fraction loading control). [See online article for color version of this figure.]

Previous studies in mammals and yeast identified ESCRT-III subunits as four small coiled-coil proteins, with their C terminus acting as the autoinhibition domain (Babst et al., 2002b; Bajorek et al., 2009). Based on the structural information and homology analyses, we generated a series of dominant negative plant ESCRT-III mutants and monitored their effects on the trafficking of four PVC/MVB cargoes (Figs. 2–4). We have shown that these ESCRT-III mutants were able to reduce the number of PVC/MVB's internal vesicles and disturb the trafficking of two membrane proteins (EMP12-GFP and LRR84A-GFP) to the internal vesicles of PVC/MVB for vacuolar degradation (Cai et al., 2012; Gao et al., 2012), resulting in their redistributions onto the outer membrane of the PVC/MVB and tonoplast of the LV (Figs. 2, 3, and 7; Table I). A recent study also highlighted a role of the ESCRT-1 complex in plant immunity via regulating endosomal sorting of FLAGELLIN SENSING2 (Spallek et al., 2013), a PM-localized receptor that perceives the bacterial flagellin (flg22) and is required for immunity against bacteria (Boller and Felix, 2009). Previous interaction analysis has revealed an ordered network of plant ESCRT-III subunits as being VPS20.1-SNF7.1-VPS24.1-VPS2.1 (Richardson et al., 2011; Shahriari et al., 2011). In addition, membrane disassociation of plant ESCRT-III subunits, but not members of the putative plant ESCRT-I and ESCRT-II subcomplexes, was regulated by the AAA ATPase SKD1 via direct interaction among VPS20.1, SNF7.1, VPS2.1, and SKD1 (Fig. 9; Supplemental Fig. S13; Katsiarimpa et al., 2011; Richardson et al., 2011), which has also been described in mammalian and yeast cells (von Schwedler et al., 2003; Yeo et al., 2003; Bowers et al., 2004; Fujita et al., 2004; Lin et al., 2005). In our study, we have systematically analyzed the ESCRT-III components by examining the effects of ESCRT-III mutants in controlling cargo sorting on the PVCs/MVBs, therefore providing direct evidence to show that conserved ESCRT-III machinery is functionally operating in plants (Fig. 10), even though plant-specific ESCRT components may exist,

such as POSITIVE REGULATOR OF SKD1, which has been identified recently (Reyes et al., 2014).

The Plant ESCRT-III Complex Associates with Scission of PVC/MVB's Internal Vesicles

The exact role of plant ESCRT complexes in luminal vesicle formation, which is topologically distinct from the classical vesicle budding events, remains largely unknown. Previous in vitro studies showed that combined action of ESCRT-I and ESCRT-II complexes deformed the membrane into buds, while the ESCRT-III complex localized to the bud neck and formed polymers to catalyze the late steps in budding and thus help the generation of intralumenal vesicles in MVBs (Ghazi-Tabatabai et al., 2008; Hanson et al., 2008; Lata et al., 2008; Wollert and Hurley, 2010). Thus, ESCRT-III subunits function as a scission machine in which SNF7 acts as the main engine (Wollert et al., 2009).

In this study, overexpression of ESCRT-III dominant negative mutants caused the reduction of PVC/MVB's intraluminal vesicles, with a much higher percentage of the vesicles remaining associated with the limiting membrane of PVC/MVB (Fig. 7; Table I). These findings are consistent with a previous study showing that overexpression of SKD1(E232Q) delayed the release of PVC/MVB's internal vesicles (Haas et al., 2007). Despite topological differences between classical vesicle and PVC/MVB's internal vesicle budding, their underlying molecular machinery may share some common features. In garland cells of *shibire*, a temperature-sensitive mutant of dynamin, which plays a key role in scission of the clathrin-coated vesicles (Wu et al., 2010; Dannhauser and Ungewickell, 2012), displayed elongated tubular intermediates and buds on the PM (Kosaka and Ikeda, 1983). Therefore, our in vivo data in Arabidopsis root cells strongly suggest that the plant ESCRT-III complex is associated with the scission of PVC/MVB's internal vesicles.

Membrane Protein Quantity and Quality Control by the ESCRT-Dependent and PVC/MVB-Mediated Vacuolar Degradation

Central to membrane protein quantity and quality control is protein degradation from the targeted membrane. In the plant endomembrane system, nascent polypeptides with significant defects are frequently retained in the endoplasmic reticulum (ER) and subjected to ER-associated degradation (Brandizzi et al., 2003; Müller et al., 2005; Hong et al., 2008; Marshall et al., 2008; Cui et al., 2012). In addition, however, post-ER compartments will change their protein content under specific physiological conditions and remove the mistargeted/misfolded proteins. In plant cells, the recent identification of several cell surface receptors/transporters as PVC/MVB luminal cargoes indicated that PVC/MVB-mediated vacuolar degradation may be a major pathway for the removal of excess PM proteins in response to different environmental conditions (Robatzek et al., 2006; Viotti et al., 2010; Barberon et al., 2011; Kasai et al., 2011; Nimchuk et al., 2011). Our results have showed that degradation of a PM cargo LRR84A in the LV is ESCRT-III dependent. Additionally, we have showed that the ESCRT-III complex plays a role in controlling abnormal cargo proteins. EMP12 is localized to

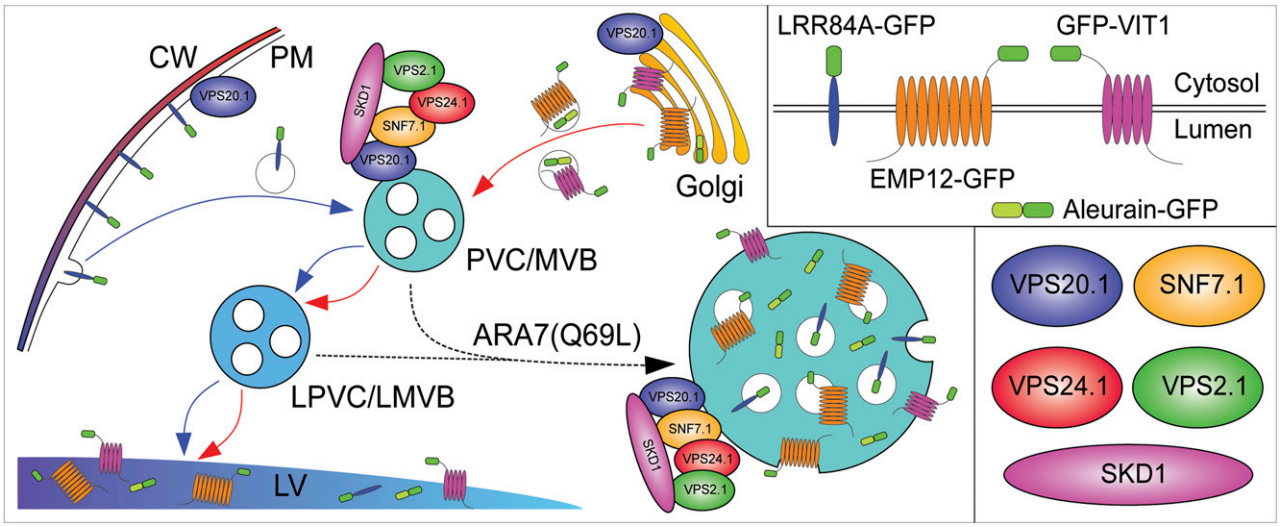

Figure 10. Schematic working model of ESCRT-III function on the PVC/MVB. Four marker proteins, aleurain-GFP, GFP-VIT1, LRR84A-GFP, and EMP12-GFP, reach the LV via the PVC/MVB from secretory or endocytic pathways. The ESCRT-III complex and its regulator SKD1 function on the PVC/MVB to sequester specific membrane cargoes and generate luminal vesicles. ER and TGN are omitted from the model for clarity. CW, Cell wall; LPVC, late prevacuolar compartment. [See online article for color version of this figure.]

the Golgi apparatus because its C-terminal KXD/E motif interacts with coat protein complex I subunits, whereas EMP12-GFP is mistargeted and delivered to the vacuole for degradation, owing to the blockage of the Golgi retention signal KXD/E by the C-terminally fused GFP (Gao et al., 2012, 2014). Our results showed that the ESCRT-III mutants disrupted the sorting of EMP12-GFP into PVCs/MVBs, implying that the ESCRT machinery was responsible for regulating vacuolar degradation of mistargeted proteins. Moreover, several other membrane proteins such as SCAMP1 and AtPRA1.B6 (for *Arabidopsis thaliana* Prenylated Rab Acceptor 1-B6) were relocated to the internal vesicles of the PVCs/MVBs when the targeting signals for post-ER compartments were deleted (Cai et al., 2011; Jung et al., 2011). Therefore, we hypothesize that ESCRT-dependent and PVC/MVB-mediated vacuolar degradation plays a major role in membrane protein quantity and quality control for post-ER compartments in plant cells (Fig. 10).

MATERIALS AND METHODS

General methods for construction and characterization of recombinant plasmids and maintenance of suspension-cultured Arabidopsis (*Arabidopsis thaliana*) plant system biology dark type culture cells have been described previously (Wang et al., 2010a, 2010b).

Plasmid Construction

For transient expression, ESCRT-III subunits and ESCRT-III mutant constructs were prepared in a pBI221 vector that contained the 35S promoter, the nopaline synthase 3′ terminator, and the CFP/MYC/YFP gene (summarized in Supplemental Table S1). For plant transformation, ESCRT-III mutants were cloned into the pER8 vector containing the LexA operator sequence fused upstream of the −46 35S minimal promoter and the Rubisco *rbcs*S3A poly(A) addition sequence (summarized in Supplemental Table S1). ESCRT-III subunits and ESCRT-III mutants were generated by PCR, double digested with their specific restriction enzymes, and inserted into the pBI221 or pER8 vector.

Transient Expression in Protoplasts, Confocal Imaging, and Colocalization Analysis

Transient expression in Arabidopsis plant system biology dark type culture and tobacco (*Nicotiana tabacum*) BY-2 protoplasts was carried out essentially as described previously (Miao and Jiang, 2007). Confocal fluorescent images were acquired 16 to 18 h after transformation in most of the experiments or 6 to 8 h during RFP-ARA7(Q69L) coexpression using an Olympus FV1000 system (http://www.olympusconfocal.com). Line-sequential scanning mode was always selected in dual-channel observation to avoid the possible cross talk between two fluorophores. For each experiment or construct, more than 30 individual cells were observed for confocal imaging that represented more than 75% of the cells showing similar expression levels and patterns. Images were processed using Adobe Photoshop software (http://www.adobe.com) as previously described (Jiang and Rogers, 1998). Colocalizations between two fluorophores were calculated by using ImageJ program with the Pearson and Spearman Correlation coefficients colocalization plug-in (French et al., 2008). Results are presented either as Pearson correlation coefficients or as Spearman's rank correlation coefficients, both of which produce r values in the range –1 to +1, where 0 indicates no discernable correlation and +1 and –1 indicate strong positive or negative correlations, respectively.

Transient Expression in Tobacco BY-2 Cells

Tobacco BY-2 cells were subcultured twice a week in liquid Murashige and Skoog (MS) medium. Three-day-cultured tobacco BY-2 cells were collected and treated with 3% (w/v) cellulysin in MS liquid medium (pH 5.7) for 45 min to loosen the cell wall. Cells were washed twice with electroporation buffer (30% [w/v] Suc, 2.4 g L^{-1} HEPES; 6 g L^{-1} KCL; and 600 mg L^{-1} $CaCl_2 \cdot 2H_2O$, pH 7.2). Ten to twenty micrograms of each construct was mixed together and incubated with the cells for 15 min before electroporation at 130 V and 1,000 μF. Cells were supplied with 5 mL of MS liquid medium and incubated for 16 to 18 h before confocal imaging.

Antibodies

GFP antibodies were purchased from Molecular Probes (catalog no. A-11122) or generated using recombinant GFP purchased from Roche Applied Science (http://www.roche-applied-science.com; catalog no. 11814524001) as antigen to inject rabbits at the Chinese University of Hong Kong. VSR antibodies were generated using AtVSR1 N-terminal recombinant protein expressed in *Drosophila melanogaster* S2 cells (Tse et al., 2004). Antibodies were affinity purified using CNBr-activated Sepharose (Sigma-Aldrich) conjugated with recombinant GFP. For western-blot analysis, GFP antibodies were used at a concentration of 4 μg mL^{-1}.

Electron Microscope Studies of Resin-Embedded Cells

The general procedures used for the preparation of transmission electron microscopy samples and thin sectioning of samples were described previously (Ritzenthaler et al., 2002; Tse et al., 2004; Wang et al., 2007, 2011, 2012; Zhuang et al., 2013). For chemical fixation, cotyledons were cut into small cubes (<1 mm) and fixed in primary fixation solution (2% [w/v] glutaraldehyde and 10% [w/v] picric acid in 25 mM CaCo buffer, pH 7.2) at 4°C overnight. After washing in CaCo buffer, samples were incubated in secondary fixation solution (2% [w/v] osmium tetroxide and 0.5% [w/v] potassium ferricyanide in 25 mM CaCo buffer, pH 7.2), followed by steps of dehydration and infiltration before embedding in Spurr's resin. Ultrathin sections were poststained with uranyl acetate/lead citrate before electron microscope (EM) observation. For high-pressure freezing, Arabidopsis roots were cut from the seedlings and immediately frozen in a high-pressure freezing apparatus (EM PACT2, Leica, http://www.leica-microsystems.com). For immunolabeling, standard procedures were performed as described previously (Lam et al., 2007a; Wang et al., 2010a, 2010b, 2013a, 2013b using anti-GFP and anti-VSR at 100 μg mL^{-1} and gold-coupled secondary antibodies with 1:50 dilution. Ultrathin sections were poststained with uranyl acetate/lead citrate before EM observation using a Hitachi H-7650 transmission EM with a CCD camera operating at 80 kV (Hitachi High-Technologies Corporation, http://www.hitachi-hitec.com/).

Protein Extraction and Immunoblot Analysis

To prepare cell extracts from protoplasts, transformed protoplasts were first diluted 3-fold with 250 mM NaCl and then harvested by centrifugation at 100g for 10 min, followed by resuspension with lysis buffer containing 25 mM Tris-HCl, pH 7.5, 150 mM NaCl, 1 mM EDTA, 1 mM phenylmethylsulphonyl fluoride, and 25 mg mL^{-1} of leupeptin. The protoplasts were further lysed by passing through a 1-mL syringe with a needle and then spun at 600g for 3 min to remove intact cells and large cellular debris. The supernatants, containing total cell extracts, were then centrifuged at 100,000g for 30 min at 4°C; the supernatant and pellet were the soluble and membrane fractions, respectively. Proteins were separated by SDS-PAGE and analyzed by immunoblotting. Quantification of the relative grayscale intensity in the immunoblots was performed using ImageJ software version 1.45 according to online instructions (http://www.lukemiller.org/index.php/2010/11/analyzing-gels-and-western-blots-with-image-j/).

FRET Measurements

FRET signals between CFP and YFP fusions were detected according to the fluorescence spectral analysis (Shah et al., 2001, 2002). Protoplasts cotransfected with CFP and YFP fusions were used for emission spectrum analysis with the Leica TCS SP5 MP confocal system. CFP and YFP images were observed in two detection channels using the 458- and 515-nm argon laser lines, respectively, as the excitation light source. For emission spectrum analysis, the 458-nm argon laser line was used as the excitation source, and excitation and emission lights were split using the Acousto-Optical Beam Splitter. The emission spectra were recorded from 464 to 600 nm with a bandwidth of 5 nm in the λ stack acquisition mode. The emission peaks at 476 and 522 nm from different regions of interest were recorded for FRET analysis by calculating

YFP/CFP fluorescence emission ratios. Free CFP and YFP were coexpressed as a negative control for the FRET analysis. For the positive control, an 18-amino acid linker peptide, SSSELSGDEVGGTSGSEF, was used to fuse the C terminus of CFP and the N terminus of YFP to create the CFP-YFP fusion (Tyas et al., 2000).

The Arabidopsis Genome Initiative locus identifiers for the genes mentioned in this article are VPS20.1 (At5g09260), SNF7.1 (At4g29160), VPS24.1 (At5g22950), VPS2.1 (At2g06530), SKD1/VPS4 (At2g27600), VPS28a (At4g21560), and VPS25 (At4g19003).

Supplemental Data

The following materials are available in the online version of this article.

Supplemental Figure S1. Subcellular localizations of VPS20.1-YFP.

Supplemental Figure S2. Subcellular localizations of SNF7.1-YFP.

Supplemental Figure S3. Subcellular localizations of VPS24.1-YFP.

Supplemental Figure S4. Subcellular localizations of VPS2.1-YFP.

Supplemental Figure S5. Overexpression of SNF7.1-YFP-induced aggregates.

Supplemental Figure S6. Coexpression of ESCRT-III subunits did not change the expression pattern of the reporters on the LV.

Supplemental Figure S7. Coexpression of ESCRT-III subunits did not change the expression pattern of the reporters on the enlarged PVC/MVB.

Supplemental Figure S8. Statistic analysis on the expression pattern of EMP12-GFP or LRR84A-GFP with coexpression of ESCRT-III dominant negative mutants.

Supplemental Figure S9. Coexpression of Arabidopsis ESCRT-III dominant negative mutants altered the expression pattern of EMP12-GFP in tobacco BY-2 cells.

Supplemental Figure S10. Effect of VPS20.1-1-112 overexpression on the localizations of ESCRT-III subunits.

Supplemental Figure S11. Coexpression of ESCRT-III mutants with GFP-VSR2 and RFP-ARA7(Q69L).

Supplemental Figure S12. Wild-type or transgenic Arabidopsis plants grown on MS plates without inducer.

Supplemental Figure S13. SKD1(E232Q) directly interacts with ESCRT-III subunits.

Supplemental Table S1. Detailed information and primer sequences for each construct.

ACKNOWLEDGMENTS

We thank Akihiko Nakano and Takashi Ueda (University of Tokyo) for providing the complementary DNA encoding ARA7(Q69L).

Received February 22, 2014; accepted May 5, 2014; published May 8, 2014.

LITERATURE CITED

Ariumi Y, Kuroki M, Maki M, Ikeda M, Dansako H, Wakita T, Kato N (2011) The ESCRT system is required for hepatitis C virus production. PLoS ONE **6:** e14517

Azmi IF, Davies BA, Xiao J, Babst M, Xu Z, Katzmann DJ (2008) ESCRT-III family members stimulate Vps4 ATPase activity directly or via Vta1. Dev Cell **14:** 50–61

Babst M, Katzmann DJ, Estepa-Sabal EJ, Meerloo T, Emr SD (2002a) Escrt-III: an endosome-associated heterooligomeric protein complex required for mvb sorting. Dev Cell **3:** 271–282

Babst M, Katzmann DJ, Snyder WB, Wendland B, Emr SD (2002b) Endosome-associated complex, ESCRT-II, recruits transport machinery for protein sorting at the multivesicular body. Dev Cell **3:** 283–289

Babst M, Sato TK, Banta LM, Emr SD (1997) Endosomal transport function in yeast requires a novel AAA-type ATPase, Vps4p. EMBO J **16:** 1820–1831

Babst M, Wendland B, Estepa EJ, Emr SD (1998) The Vps4p AAA ATPase regulates membrane association of a Vps protein complex required for normal endosome function. EMBO J **17:** 2982–2993

Bajorek M, Schubert HL, McCullough J, Langelier C, Eckert DM, Stubblefield WM, Uter NT, Myszka DG, Hill CP, Sundquist WI (2009) Structural basis for ESCRT-III protein autoinhibition. Nat Struct Mol Biol **16:** 754–762

Barberon M, Zelazny E, Robert S, Conéjéro G, Curie C, Friml J, Vert G (2011) Monoubiquitin-dependent endocytosis of the iron-regulated transporter 1 (IRT1) transporter controls iron uptake in plants. Proc Natl Acad Sci USA **108:** E450–E458

Bilodeau PS, Urbanowski JL, Winistorfer SC, Piper RC (2002) The Vps27p Hse1p complex binds ubiquitin and mediates endosomal protein sorting. Nat Cell Biol **4:** 534–539

Bilodeau PS, Winistorfer SC, Kearney WR, Robertson AD, Piper RC (2003) Vps27-Hse1 and ESCRT-I complexes cooperate to increase efficiency of sorting ubiquitinated proteins at the endosome. J Cell Biol **163:** 237–243

Boller T, Felix G (2009) A renaissance of elicitors: perception of microbe-associated molecular patterns and danger signals by pattern-recognition receptors. Annu Rev Plant Biol **60:** 379–406

Bowers K, Lottridge J, Helliwell SB, Goldthwaite LM, Luzio JP, Stevens TH (2004) Protein-protein interactions of ESCRT complexes in the yeast *Saccharomyces cerevisiae*. Traffic **5:** 194–210

Brandizzi F, Frangne N, Marc-Martin S, Hawes C, Neuhaus JM, Paris N (2002) The destination for single-pass membrane proteins is influenced markedly by the length of the hydrophobic domain. Plant Cell **14:** 1077–1092

Brandizzi F, Hanton S, DaSilva LLP, Boevink P, Evans D, Oparka K, Denecke J, Hawes C (2003) ER quality control can lead to retrograde transport from the ER lumen to the cytosol and the nucleoplasm in plants. Plant J **34:** 269–281

Cai Y, Jia T, Lam SK, Ding Y, Gao C, San MW, Pimpl P, Jiang L (2011) Multiple cytosolic and transmembrane determinants are required for the trafficking of SCAMP1 via an ER-Golgi-TGN-PM pathway. Plant J **65:** 882–896

Cai Y, Zhuang X, Wang J, Wang H, Lam SK, Gao C, Wang X, Jiang L (2012) Vacuolar degradation of two integral plasma membrane proteins, AtLRR84A and OsSCAMP1, is cargo ubiquitination-independent and prevacuolar compartment-mediated in plant cells. Traffic **13:** 1023–1040

Carlton JG, Caballe A, Agromayor M, Kloc M, Martin-Serrano J (2012) ESCRT-III governs the Aurora B-mediated abscission checkpoint through CHMP4C. Science **336:** 220–225

Chow CM, Neto H, Foucart C, Moore I (2008) Rab-A2 and Rab-A3 GTPases define a *trans*-golgi endosomal membrane domain in *Arabidopsis* that contributes substantially to the cell plate. Plant Cell **20:** 101–123

Cui F, Liu L, Zhao Q, Zhang Z, Li Q, Lin B, Wu Y, Tang S, Xie Q (2012) *Arabidopsis* ubiquitin conjugase UBC32 is an ERAD component that functions in brassinosteroid-mediated salt stress tolerance. Plant Cell **24:** 233–244

Cui Y, Zhao Q, Gao C, Ding Y, Zeng Y, Ueda T, Nakano A, Jiang L (May 13, 2014) Activation of the Rab7 GTPase by the MON1-CCZ1 complex is essential for PVC-to-vacuole trafficking and plant growth in *Arabidopsis*. Plant Cell http://dx.doi.org/10.1105/tpc.114.123141

Dannhauser PN, Ungewickell EJ (2012) Reconstitution of clathrin-coated bud and vesicle formation with minimal components. Nat Cell Biol **14:** 634–639

daSilva LL, Foresti O, Denecke J (2006) Targeting of the plant vacuolar sorting receptor BP80 is dependent on multiple sorting signals in the cytosolic tail. Plant Cell **18:** 1477–1497

daSilva LL, Taylor JP, Hadlington JL, Hanton SL, Snowden CJ, Fox SJ, Foresti O, Brandizzi F, Denecke J (2005) Receptor salvage from the prevacuolar compartment is essential for efficient vacuolar protein targeting. Plant Cell **17:** 132–148

Davies BA, Azmi IF, Payne J, Shestakova A, Horazdovsky BF, Babst M, Katzmann DJ (2010) Coordination of substrate binding and ATP hydrolysis in Vps4-mediated ESCRT-III disassembly. Mol Biol Cell **21:** 3396–3408

Denecke J, Aniento F, Frigerio L, Hawes C, Hwang I, Mathur J, Neuhaus JM, Robinson DG (2012) Secretory pathway research: the more experimental systems the better. Plant Cell **24:** 1316–1326

Ding Y, Wang J, Wang J, Stierhof YD, Robinson DG, Jiang L (2012) Unconventional protein secretion. Trends Plant Sci **17:** 606–615

Dukes JD, Richardson JD, Simmons R, Whitley P (2008) A dominant-negative ESCRT-III protein perturbs cytokinesis and trafficking to lysosomes. Biochem J **411:** 233–239

Foresti O, Denecke J (2008) Intermediate organelles of the plant secretory pathway: identity and function. Traffic **9:** 1599–1612

Foresti O, Gershlick DC, Bottanelli F, Hummel E, Hawes C, Denecke J (2010) A recycling-defective vacuolar sorting receptor reveals an intermediate compartment situated between prevacuoles and vacuoles in tobacco. Plant Cell **22:** 3992–4008

French AP, Mills S, Swarup R, Bennett MJ, Pridmore TP (2008) Colocalization of fluorescent markers in confocal microscope images of plant cells. Nat Protoc **3:** 619–628

Frigerio L, Foresti O, Felipe DH, Neuhaus JM, Vitale A (2001) The C-terminal tetrapeptide of phaseolin is sufficient to target green fluorescent protein to the vacuole. J Plant Physiol **158:** 499–503

Fujita H, Umezuki Y, Imamura K, Ishikawa D, Uchimura S, Nara A, Yoshimori T, Hayashizaki Y, Kawai J, Ishidoh K, et al (2004) Mammalian class E Vps proteins, SBP1 and mVps2/CHMP2A, interact with and regulate the function of an AAA-ATPase SKD1/Vps4B. J Cell Sci **117:** 2997–3009

Fumoto K, Kikuchi K, Gon H, Kikuchi A (2012) Wnt5a signaling controls cytokinesis by positioning ESCRT-III to the proper site at the midbody. J Cell Sci **15:** 4822–4832

Gao C, Cai Y, Wang Y, Kang BH, Aniento F, Robinson DG, Jiang L (April 30, 2014) Retention mechanisms for ER and Golgi membrane proteins. Trends Plant Sci http://dx.doi.org/10.1016/j.tplants.2014.04.004

Gao C, Yu CK, Qu S, San MW, Li KY, Lo SW, Jiang L (2012) The Golgi-localized *Arabidopsis* endomembrane protein12 contains both endoplasmic reticulum export and Golgi retention signals at its C terminus. Plant Cell **24:** 2086–2104

Ghazi-Tabatabai S, Saksena S, Short JM, Pobbati AV, Veprintsev DB, Crowther RA, Emr SD, Egelman EH, Williams RL (2008) Structure and disassembly of filaments formed by the ESCRT-III subunit Vps24. Structure **16:** 1345–1356

Guizetti J, Schermelleh L, Mäntler J, Maar S, Poser I, Leonhardt H, Müller-Reichert T, Gerlich DW (2011) Cortical constriction during abscission involves helices of ESCRT-III-dependent filaments. Science **331:** 1616–1620

Haas TJ, Sliwinski MK, Martínez DE, Preuss M, Ebine K, Ueda T, Nielsen E, Odorizzi G, Otegui MS (2007) The *Arabidopsis* AAA ATPase SKD1 is involved in multivesicular endosome function and interacts with its positive regulator LYST-INTERACTING PROTEIN5. Plant Cell **19:** 1295–1312

Hanson PI, Roth R, Lin Y, Heuser JE (2008) Plasma membrane deformation by circular arrays of ESCRT-III protein filaments. J Cell Biol **180:** 389–402

Henne WM, Buchkovich NJ, Emr SD (2011) The ESCRT pathway. Dev Cell **21:** 77–91

Henne WM, Buchkovich NJ, Zhao Y, Emr SD (2012) The endosomal sorting complex ESCRT-II mediates the assembly and architecture of ESCRT-III helices. Cell **151:** 356–371

Hislop JN, von Zastrow M (2011) Role of ubiquitination in endocytic trafficking of G-protein-coupled receptors. Traffic **12:** 137–148

Hong Z, Jin H, Tzfira T, Li J (2008) Multiple mechanism-mediated retention of a defective brassinosteroid receptor in the endoplasmic reticulum of *Arabidopsis*. Plant Cell **20:** 3418–3429

Hurley JH, Emr SD (2006) The ESCRT complexes: structure and mechanism of a membrane-trafficking network. Annu Rev Biophys Biomol Struct **35:** 277–298

Hurley JH, Hanson PI (2010) Membrane budding and scission by the ESCRT machinery: it's all in the neck. Nat Rev Mol Cell Biol **11:** 556–566

Hwang I (2008) Sorting and anterograde trafficking at the Golgi apparatus. Plant Physiol **148:** 673–683

Ibl V, Csaszar E, Schlager N, Neubert S, Spitzer C, Hauser MT (2012) Interactome of the plant-specific ESCRT-III component AtVPS2.2 in *Arabidopsis thaliana*. J Proteome Res **11:** 397–411

Jia T, Gao C, Cui Y, Wang J, Ding Y, Cai Y, Ueda T, Nakano A, Jiang L (2013) ARA7(Q69L) expression in transgenic Arabidopsis cells induces the formation of enlarged multivesicular bodies. J Exp Bot **64:** 2817–2829

Jiang L, Rogers JC (1998) Integral membrane protein sorting to vacuoles in plant cells: evidence for two pathways. J Cell Biol **143:** 1183–1199

Jung CJ, Lee MH, Min MK, Hwang I (2011) Localization and trafficking of an isoform of the AtPRA1 family to the Golgi apparatus depend on both N- and C-terminal sequence motifs. Traffic **12:** 185–200

Kang BH, Nielsen E, Preuss ML, Mastronarde D, Staehelin LA (2011) Electron tomography of RabA4b- and PI-4Kβ1-labeled trans Golgi network compartments in Arabidopsis. Traffic **12:** 313–329

Kasai K, Takano J, Miwa K, Toyoda A, Fujiwara T (2011) High boron-induced ubiquitination regulates vacuolar sorting of the BOR1 borate transporter in *Arabidopsis thaliana*. J Biol Chem **286:** 6175–6183

Katsiarimpa A, Anzenberger F, Schlager N, Neubert S, Hauser MT, Schwechheimer C, Isono E (2011) The *Arabidopsis* deubiquitinating enzyme AMSH3 interacts with ESCRT-III subunits and regulates their localization. Plant Cell **23:** 3026–3040

Katsiarimpa A, Kalinowska K, Anzenberger F, Weis C, Ostertag M, Tsutsumi C, Schwechheimer C, Brunner F, Hückelhoven R, Isono E (2013) The deubiquitinating enzyme AMSH1 and the ESCRT-III subunit VPS2.1 are required for autophagic degradation in *Arabidopsis*. Plant Cell **25:** 2236–2252

Katzmann DJ, Babst M, Emr SD (2001) Ubiquitin-dependent sorting into the multivesicular body pathway requires the function of a conserved endosomal protein sorting complex, ESCRT-I. Cell **106:** 145–155

Katzmann DJ, Stefan CJ, Babst M, Emr SD (2003) Vps27 recruits ESCRT machinery to endosomes during MVB sorting. J Cell Biol **162:** 413–423

Kim SA, Punshon T, Lanzirotti A, Li L, Alonso JM, Ecker JR, Kaplan J, Guerinot ML (2006) Localization of iron in Arabidopsis seed requires the vacuolar membrane transporter VIT1. Science **314:** 1295–1298

Komarova NY, Meier S, Meier A, Grotemeyer MS, Rentsch D (2012) Determinants for Arabidopsis peptide transporter targeting to the tonoplast or plasma membrane. Traffic **13:** 1090–1105

Kosaka T, Ikeda K (1983) Reversible blockage of membrane retrieval and endocytosis in the garland cell of the temperature-sensitive mutant of *Drosophila melanogaster*, shibirets1. J Cell Biol **97:** 499–507

Kostelansky MS, Sun J, Lee S, Kim J, Ghirlando R, Hierro A, Emr SD, Hurley JH (2006) Structural and functional organization of the ESCRT-I trafficking complex. Cell **125:** 113–126

Kotzer AM, Brandizzi F, Neumann U, Paris N, Moore I, Hawes C (2004) AtRabF2b (Ara7) acts on the vacuolar trafficking pathway in tobacco leaf epidermal cells. J Cell Sci **117:** 6377–6389

Lam SK, Siu CL, Hillmer S, Jang S, An G, Robinson DG, Jiang L (2007a) Rice SCAMP1 defines clathrin-coated, *trans*-golgi-located tubular-vesicular structures as an early endosome in tobacco BY-2 cells. Plant Cell **19:** 296–319

Lam SK, Tse YC, Robinson DG, Jiang L (2007b) Tracking down the elusive early endosome. Trends Plant Sci **12:** 497–505

Larisch N, Schulze C, Galione A, Dietrich P (2012) An N-terminal dileucine motif directs two-pore channels to the tonoplast of plant cells. Traffic **13:** 1012–1022

Lata S, Schoehn G, Jain A, Pires R, Piehler J, Gottlinger HG, Weissenhorn W (2008) Helical structures of ESCRT-III are disassembled by VPS4. Science **321:** 1354–1357

Le Bras S, Loyer N, Le Borgne R (2011) The multiple facets of ubiquitination in the regulation of notch signaling pathway. Traffic **12:** 149–161

Leung KF, Dacks JB, Field MC (2008) Evolution of the multivesicular body ESCRT machinery; retention across the eukaryotic lineage. Traffic **9:** 1698–1716

Liang Y, Wang X, Hong S, Li Y, Zuo J (2012) Deletion of the initial 45 residues of ARR18 induces cytokinin response in Arabidopsis. J Genet Genomics **39:** 37–46

Lin Y, Kimpler LA, Naismith TV, Lauer JM, Hanson PI (2005) Interaction of the mammalian endosomal sorting complex required for transport (ESCRT) III protein hSnf7-1 with itself, membranes, and the AAA^+ ATPase SKD1. J Biol Chem **280:** 12799–12809

Marshall RS, Jolliffe NA, Ceriotti A, Snowden CJ, Lord JM, Frigerio L, Roberts LM (2008) The role of CDC48 in the retro-translocation of non-ubiquitinated toxin substrates in plant cells. J Biol Chem **283:** 15869–15877

McMurray MA, Stefan CJ, Wemmer M, Odorizzi G, Emr SD, Thorner J (2011) Genetic interactions with mutations affecting septin assembly reveal ESCRT functions in budding yeast cytokinesis. Biol Chem **392:** 699–712

Miao Y, Jiang L (2007) Transient expression of fluorescent fusion proteins in protoplasts of suspension cultured cells. Nat Protoc **2:** 2348–2353

Müller J, Mettbach U, Menzel D, Samaj J (2007) Molecular dissection of endosomal compartments in plants. Plant Physiol **145:** 293–304

Müller J, Piffanelli P, Devoto A, Miklis M, Elliott C, Ortmann B, Schulze-Lefert P, Panstruga R (2005) Conserved ERAD-like quality control of a plant polytopic membrane protein. Plant Cell **17:** 149–163

Nimchuk ZL, Tarr PT, Ohno C, Qu X, Meyerowitz EM (2011) Plant stem cell signaling involves ligand-dependent trafficking of the CLAVATA1 receptor kinase. Curr Biol **21:** 345–352

Odorizzi G, Babst M, Emr SD (1998) Fab1p PtdIns(3)P 5-kinase function essential for protein sorting in the multivesicular body. Cell **95:** 847–858
Otegui MS, Spitzer C (2008) Endosomal functions in plants. Traffic **9:** 1589–1598
Piper RC, Cooper AA, Yang H, Stevens TH (1995) VPS27 controls vacuolar and endocytic traffic through a prevacuolar compartment in *Saccharomyces cerevisiae*. J Cell Biol **131:** 603–617
Reyes FC, Buono RA, Roschzttardtz H, Di Rubbo S, Yeun LH, Russinova E, Otegui MS (2014) A novel endosomal sorting complex required for transport (ESCRT) component in *Arabidopsis thaliana* controls cell expansion and development. J Biol Chem **289:** 4980–4988
Richardson LG, Howard AS, Khuu N, Gidda SK, McCartney A, Morphy BJ, Mullen RT (2011) Protein-protein interaction network and subcellular localization of the *Arabidopsis thaliana* ESCRT machinery. Front Plant Sci **2:** 20
Richter S, Voss U, Jürgens G (2009) Post-Golgi traffic in plants. Traffic **10:** 819–828
Ritzenthaler C, Nebenführ A, Movafeghi A, Stussi-Garaud C, Behnia L, Pimpl P, Staehelin LA, Robinson DG (2002) Reevaluation of the effects of brefeldin A on plant cells using tobacco Bright Yellow 2 cells expressing Golgi-targeted green fluorescent protein and COPI antisera. Plant Cell **14:** 237–261
Robatzek S, Chinchilla D, Boller T (2006) Ligand-induced endocytosis of the pattern recognition receptor FLS2 in Arabidopsis. Genes Dev **20:** 537–542
Robinson DG, Jiang L, Schumacher K (2008) The endosomal system of plants: charting new and familiar territories. Plant Physiol **147:** 1482–1492
Saksena S, Wahlman J, Teis D, Johnson AE, Emr SD (2009) Functional reconstitution of ESCRT-III assembly and disassembly. Cell **136:** 97–109
Schellmann S, Pimpl P (2009) Coats of endosomal protein sorting: retromer and ESCRT. Curr Opin Plant Biol **12:** 670–676
Scheuring D, Viotti C, Krüger F, Künzl F, Sturm S, Bubeck J, Hillmer S, Frigerio L, Robinson DG, Pimpl P, et al (2011) Multivesicular bodies mature from the *trans*-Golgi network/early endosome in *Arabidopsis*. Plant Cell **23:** 3463–3481
Schiel JA, Simon GC, Zaharris C, Weisz J, Castle D, Wu CC, Prekeris R (2012) FIP3-endosome-dependent formation of the secondary ingression mediates ESCRT-III recruitment during cytokinesis. Nat Cell Biol **14:** 1068–1078
Shah K, Gadella TW Jr, van Erp H, Hecht V, de Vries SC (2001) Subcellular localization and oligomerization of the *Arabidopsis thaliana* somatic embryogenesis receptor kinase 1 protein. J Mol Biol **309:** 641–655
Shah K, Russinova E, Gadella TW Jr, Willemse J, De Vries SC (2002) The Arabidopsis kinase-associated protein phosphatase controls internalization of the somatic embryogenesis receptor kinase 1. Genes Dev **16:** 1707–1720
Shahriari M, Keshavaiah C, Scheuring D, Sabovljevic A, Pimpl P, Häusler RE, Hülskamp M, Schellmann S (2010) The AAA-type ATPase AtSKD1 contributes to vacuolar maintenance of *Arabidopsis thaliana*. Plant J **64:** 71–85
Shahriari M, Richter K, Keshavaiah C, Sabovljevic A, Huelskamp M, Schellmann S (2011) The Arabidopsis ESCRT protein-protein interaction network. Plant Mol Biol **76:** 85–96
Shen J, Zeng Y, Zhuang X, Sun L, Yao X, Pimpl P, Jiang L (2013) Organelle pH in the Arabidopsis endomembrane system. Mol Plant **6:** 1419–1437
Shields SB, Piper RC (2011) How ubiquitin functions with ESCRTs. Traffic **12:** 1306–1317
Spallek T, Beck M, Ben Khaled S, Salomon S, Bourdais G, Schellmann S, Robatzek S (2013) ESCRT-I mediates FLS2 endosomal sorting and plant immunity. PLoS Genet **9:** e1004035
Spitzer C, Reyes FC, Buono R, Sliwinski MK, Haas TJ, Otegui MS (2009) The ESCRT-related CHMP1A and B proteins mediate multivesicular body sorting of auxin carriers in *Arabidopsis* and are required for plant development. Plant Cell **21:** 749–766
Spitzer C, Schellmann S, Sabovljevic A, Shahriari M, Keshavaiah C, Bechtold N, Herzog M, Müller S, Hanisch FG, Hülskamp M (2006) The Arabidopsis elch mutant reveals functions of an ESCRT component in cytokinesis. Development **133:** 4679–4689
Spormann DO, Heim J, Wolf DH (1992) Biogenesis of the yeast vacuole (lysosome). The precursor forms of the soluble hydrolase carboxypeptidase yscS are associated with the vacuolar membrane. J Biol Chem **267:** 8021–8029
Stuchell-Brereton MD, Skalicky JJ, Kieffer C, Karren MA, Ghaffarian S, Sundquist WI (2007) ESCRT-III recognition by VPS4 ATPases. Nature **449:** 740–744
Teis D, Saksena S, Emr SD (2008) Ordered assembly of the ESCRT-III complex on endosomes is required to sequester cargo during MVB formation. Dev Cell **15:** 578–589
Teis D, Saksena S, Judson BL, Emr SD (2010) ESCRT-II coordinates the assembly of ESCRT-III filaments for cargo sorting and multivesicular body vesicle formation. EMBO J **29:** 871–883
Teo H, Gill DJ, Sun J, Perisic O, Veprintsev DB, Vallis Y, Emr SD, Williams RL (2006) ESCRT-I core and ESCRT-II GLUE domain structures reveal role for GLUE in linking to ESCRT-I and membranes. Cell **125:** 99–111
Tsang HT, Connell JW, Brown SE, Thompson A, Reid E, Sanderson CM (2006) A systematic analysis of human CHMP protein interactions: additional MIT domain-containing proteins bind to multiple components of the human ESCRT III complex. Genomics **88:** 333–346
Tse YC, Mo B, Hillmer S, Zhao M, Lo SW, Robinson DG, Jiang L (2004) Identification of multivesicular bodies as prevacuolar compartments in *Nicotiana tabacum* BY-2 cells. Plant Cell **16:** 672–693
Tyas L, Brophy VA, Pope A, Rivett AJ, Tavaré JM (2000) Rapid caspase-3 activation during apoptosis revealed using fluorescence-resonance energy transfer. EMBO Rep **1:** 266–270
Urbé S (2011) Moving in with ubiquitin. Traffic **12:** 135–136
Viotti C, Bubeck J, Stierhof YD, Krebs M, Langhans M, van den Berg W, van Dongen W, Richter S, Geldner N, Takano J, et al (2010) Endocytic and secretory traffic in *Arabidopsis* merge in the *trans*-Golgi network/early endosome, an independent and highly dynamic organelle. Plant Cell **22:** 1344–1357
von Schwedler UK, Stuchell M, Müller B, Ward DM, Chung HY, Morita E, Wang HE, Davis T, He GP, Cimbora DM, et al (2003) The protein network of HIV budding. Cell **114:** 701–713
Wang H, Tse YC, Law AH, Sun SS, Sun YB, Xu ZF, Hillmer S, Robinson DG, Jiang L (2010a) Vacuolar sorting receptors (VSRs) and secretory carrier membrane proteins (SCAMPs) are essential for pollen tube growth. Plant J **61:** 826–838
Wang H, Zhuang X, Cai Y, Cheung A, Jiang L (2013a) Apical F-actin regulated exocytosis and endocytosis is essential for pectic cell wall construction and cell polarization in pollen tubes. Plant J **76:** 367–379
Wang H, Zhuang XH, Hillmer S, Robinson DG, Jiang LW (2011) Vacuolar sorting receptor (VSR) proteins reach the plasma membrane in germinating pollen tubes. Mol Plant **4:** 845–853
Wang J, Ding Y, Wang J, Hillmer S, Miao Y, Lo SW, Wang X, Robinson DG, Jiang L (2010b) EXPO, an exocyst-positive organelle distinct from multivesicular endosomes and autophagosomes, mediates cytosol to cell wall exocytosis in *Arabidopsis* and tobacco cells. Plant Cell **22:** 4009–4030
Wang J, Li Y, Lo SW, Hillmer S, Sun SS, Robinson DG, Jiang L (2007) Protein mobilization in germinating mung bean seeds involves vacuolar sorting receptors and multivesicular bodies. Plant Physiol **143:** 1628–1639
Wang J, Shen J, Cai Y, Robinson DG, Jiang L (2013b) Successful transport to the vacuole of heterologously expressed mung bean 8S globulin occurs in seed but not in vegetative tissues. J Exp Bot **64:** 1587–1601
Wang J, Tse YC, Hinz G, Robinson DG, Jiang L (2012) Storage globulins pass through the Golgi apparatus and multivesicular bodies in the absence of dense vesicle formation during early stages of cotyledon development in mung bean. J Exp Bot **63:** 1367–1380
Weiss P, Huppert S, Kölling R (2009) Analysis of the dual function of the ESCRT-III protein Snf7 in endocytic trafficking and in gene expression. Biochem J **424:** 89–97
Winter V, Hauser MT (2006) Exploring the ESCRTing machinery in eukaryotes. Trends Plant Sci **11:** 115–123
Wolfenstetter S, Wirsching P, Dotzauer D, Schneider S, Sauer N (2012) Routes to the tonoplast: the sorting of tonoplast transporters in *Arabidopsis* mesophyll protoplasts. Plant Cell **24:** 215–232
Wollert T, Hurley JH (2010) Molecular mechanism of multivesicular body biogenesis by ESCRT complexes. Nature **464:** 864–869
Wollert T, Wunder C, Lippincott-Schwartz J, Hurley JH (2009) Membrane scission by the ESCRT-III complex. Nature **458:** 172–177
Wu M, Huang B, Graham M, Raimondi A, Heuser JE, Zhuang X, De Camilli P (2010) Coupling between clathrin-dependent endocytic budding and F-BAR-dependent tubulation in a cell-free system. Nat Cell Biol **12:** 902–908
Yeo SC, Xu L, Ren J, Boulton VJ, Wagle MD, Liu C, Ren G, Wong P, Zahn R, Sasajala P, et al (2003) Vps20p and Vta1p interact with Vps4p and function in multivesicular body sorting and endosomal transport in *Saccharomyces cerevisiae*. J Cell Sci **116:** 3957–3970
Zhuang X, Wang H, Lam SK, Gao C, Wang X, Cai Y, Jiang L (2013) A BAR-domain protein SH3P2, which binds to phosphatidylinositol 3-phosphate and ATG8, regulates autophagosome formation in *Arabidopsis*. Plant Cell **25:** 4596–4615
Zuo J, Niu QW, Chua NH (2000) Technical advance: an estrogen receptor-based transactivator XVE mediates highly inducible gene expression in transgenic plants. Plant J **24:** 265–273